Journal of Medicinal Chemistry

Article

pubs.acs.org/jmc

Discovery of Dap-3 Polymyxin Analogues for the Treatment of Multidrug-Resistant Gram-Negative Nosocomial Infections

Thomas V. Magee,*[,†,#] Matthew F. Brown,[†] Jeremy T. Starr,[†] David C. Ackley,[†] Joseph A. Abramite,[†] Jiri Aubrecht,[†] Andrew Butler,[†] Jared L. Crandon,[‡] Fadia Dib-Hajj,[†] Mark E. Flanagan,[†] Karl Granskog,[†] Joel R. Hardink,[†] Michael D. Huband,[†,▽] Rebecca Irvine,[†] Michael Kuhn,[†] Karen L. Leach,[†] Bryan Li,[†] Jian Lin,[†] David R. Luke,[†] Shawn H. MacVane,[‡] Alita A. Miller,[†,▽] Sandra McCurdy,[†,○] James M. McKim, Jr.,[§] David P. Nicolau,[‡] Thuy-Trinh Nguyen,[†] Mark C. Noe,[†] John P. O'Donnell,[†,▽] Scott B. Seibel,[†] Yue Shen,[†] Antonia F. Stepan,[†] Andrew P. Tomaras,[†] Paul C. Wilga,[§] Li Zhang,[∥] Jinfeng Xu,[⊥] and Jinshan Michael Chen[†]

[†]Pfizer Worldwide Research & Development, Pfizer, Inc., Groton, Connecticut 06340, United States

[‡]Center for Anti-Infective Research and Development, Hartford Hospital, Hartford, Connecticut 06102, United States

[§]CeeTox, Inc., Kalamazoo, Michigan 49008, United States

[∥]WuXi AppTech Co., Ltd., Shanghai, P.R. China

[⊥]CPC Scientific, Hangzhou, P.R. China

ABSTRACT: We report novel polymyxin analogues with improved antibacterial in vitro potency against polymyxin resistant recent clinical isolates of *Acinetobacter baumannii* and *Pseudomonas aeruginosa*. In addition, a human renal cell in vitro assay (hRPTEC) was used to inform structure−toxicity relationships and further differentiate analogues. Replacement of the Dab-3 residue with a Dap-3 in combination with a relatively polar 6-oxo-1-phenyl-1,6-dihydropyridine-3-carbonyl side chain as a fatty acyl replacement yielded analogue **5x**, which demonstrated an improved in vitro antimicrobial and renal cytotoxicity profiles relative to polymyxin B (PMB). However, in vivo PK/PD comparison of **5x** and PMB in a murine neutropenic thigh model against *P. aeruginosa* strains with matched MICs showed that **5x** was inferior to PMB in vivo, suggesting a lack of improved therapeutic index in spite of apparent in vitro advantages.

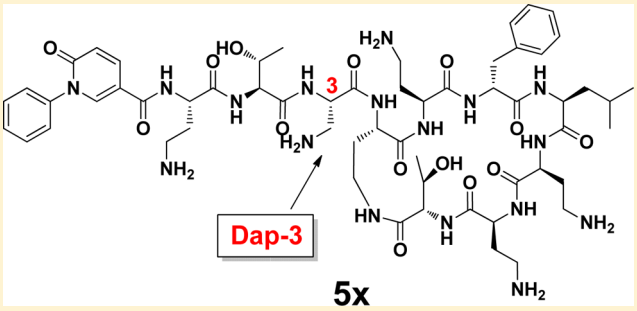

INTRODUCTION

Multidrug-resistant Gram-negative pathogens such as *Pseudomonas aeruginosa* and *Acinetobacter baumannii* are an increasing menace, particularly in hospital intensive care units, leading to an impending healthcare crisis with fewer and fewer treatment options available.[1] Although over 50 years old, the polymyxin class has made a resurgence of late in response to this crisis.[2] The polymyxins are polycationic lipodecapeptides (Figure 1), exemplified by polymyxins B (PMB) and E (more commonly known as colistin), natural product mixtures first isolated from *Bacillus polymyxa*.[3] Polymyxin B and colistin are differentiated only by the D-form amino acid in position 6 of the cyclic peptide portion of the molecule, D-Phe-6 and D-Leu-6, respectively. The major component of both mixtures contains a (*S*)-6-methyloctanoyl (polymyxin B1 and colistin A, respectively) lipophilic attachment at the α-amine of the diaminobutyric acid (Dab) residue at the N-terminal or 1-position (Dab-1).[4] Both drugs are currently used in clinical practice for treatment of serious Gram-negative infections, although colistin is almost exclusively administered in nonactive prodrug form as the pentamethanosulfonate sodium salt.[5]

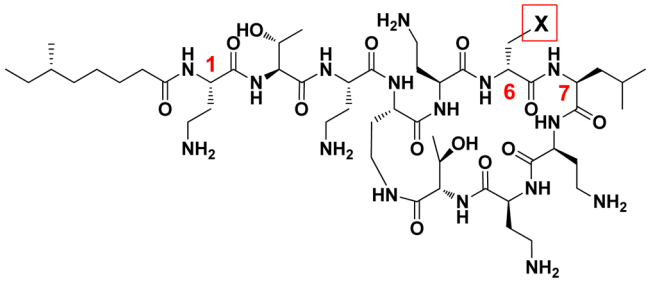

Figure 1. The major components of polymyxin B (PMB) and colistin, respectively: X = phenyl (polymyxin B1, **1**) and X = 2-propyl (colistin A, **2**).

Received: March 21, 2013
Published: June 4, 2013

The attraction of the polymyxins is their persistent potency against the multidrug-resistant nonfermenting (*P. aeruginosa*, *A. baumannii*) and enteric (*Klebsiella pneumoniae*, *Escherichia coli*) pathogens in the face of widespread carbapenem resistance.[6] Unlike β-lactams, which must penetrate the bacterial outer membrane to reach their target, survive β-lactamase hydrolysis, and avoid the activity of efflux pumps to be effective, the polymyxins act initially on the outer leaf of the outer membrane by first binding the lipid A portion of lipopolysaccharide.[7] What happens after binding lipid A is not entirely clear, although modeling suggests that polymyxins promote the exchange of phospholipids between the outer and inner membranes, creating osmotic instability and resulting in cell death.[8] What is clear is that a certain number of cationic residues are required, along with lipophilic projections from both the N-terminus and within the cyclic peptide (residues 6 and 7), which likely provide membrane anchoring and are essential for antimicrobial activity.[9] The amphipathic nature of the charge-lipophilicity distribution is an essential feature of their mode of action, although the selectivity of polymyxins for (LPS-containing) Gram-negative over Gram-positive bacteria suggests a lack of general detergent qualities often associated with amphipathic molecules. The major challenge with polycationic lipopeptides such as polymyxin is their tendency to disrupt renal and, in rare cases, neuromuscular function. Nephrotoxicity, the main concern for the polymyxins, can be quite variable and dependent upon the state and history of the patient but presents limited therapeutic and dosing options to the treating clinician. For this reason, these agents are often used as a "last resort".[10] Underdosing of polymyxins owing to these safety concerns presents the prospect of failure to eradicate the infecting pathogen for the patient and the potential for generating polymyxin resistant strains which could spread to others. To address these issues, Vaara et al. have taken the innovative approach of significantly modifying the side chain of the lipopeptide such that it no longer contains any basic residues. The resulting molecules, with an overall positive charge count reduced from five to three, act on the outer membrane to potentiate the entry of Gram-positive agents such as macrolides that would otherwise not penetrate the outer membrane of Gram-negative bacteria.[11] Interestingly, these "potentiators" still retain some intrinsic antimicrobial potency as well. Polymyxin B nonapeptide (PMBN) is the result of enzymatic cleavage of PMB, removing the fatty acyl and Dab-1 units and leaving amino acid residues 2−10 intact.[12] PMBN is also known to have relatively poor intrinsic MICs but exhibits potentiator properties.[13] Sato et al. have also modified the side chain with a *des*-fatty acyl approach and reduced the basicity to give compounds that appear to retain good intrinsic antibacterial potency against *P. aeruginosa* (but lose *E. coli* potency; *A. baumannii* and *K. pneumoniae* data not reported) with an apparent lower toxicity liability.[14] Other approaches to improving upon the polymyxins have included replacing the fatty acyl side chain with more compact entities such as an aryl urea.[15] Researchers at Monash University disclosed a patent application[16] concentrating upon extending the lipophilic residues in the cyclic peptide region, particularly at Leu-7, with long-chain hydrocarbons or biphenyl moieties and capping the N-terminus with biphenyl amide to improve potency against polymyxin resistant strains. Such resistant strains are currently rare; however, they are known[17] and are likely to grow in importance as physicians increasingly turn to polymyxins to treat these infections.

SYNTHETIC CHEMISTRY

Solid phase peptide synthesis on 2-chlorotrityl chloride (CTC) resin was used to synthesize our target compounds (Scheme 1).

Scheme 1. Synthesis of Dap-3 Polymyxin Analogues with Variable N-Termini (R) on Template 5[a]

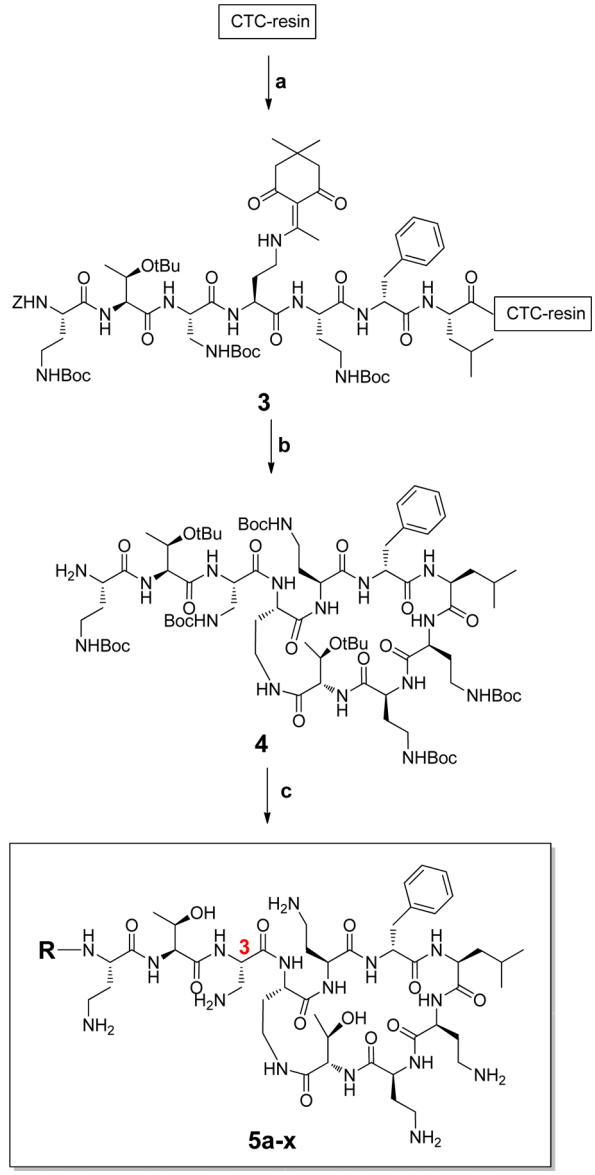

[a]Conditions: (a) (i) CTC resin, Fmoc-Leu-OH, DIPEA, DCM, MeOH; (ii) sequential removal of Fmoc (piperidine, DMF) followed by amidation (Fmoc-AA-OH, HOBt, DIC, DMF) using the following residues (resin filtration between steps): Fmoc-DPhe-OH, Fmoc-Dab(Boc)-OH, Fmoc-Dab(Dde)-OH, Fmoc-Dap(Boc)-OH, Fmoc-Thr(tBu)-OH, Fmoc-Dab(Boc)-OH; (iii) *Z*-OSu, NMM, DMF. (b) (i) 3% hydrazine in DMF to remove Dde; (ii) sequential amidation/Fmoc removal as above with: Fmoc-Thr(tBu)-OH, Fmoc-Dab(Boc)-OH, Fmoc-Dab(Boc)-OH; (iii) 1.5% TFA in DCM (resin cleavage); (iv) cyclization in DMF at 0.002 M dilution with EDC-HCl, DIPEA, 70% yield for this step; (v) H_2 (1.1 atm), cat. Pd/C, DCM, MeOH, NH_4OH. (c) (i) For amidation, carboxylic acid coupling partner, HATU, TEA, DMSO; for sulfonylation, sulfonyl chloride coupling partner, NMM, DMF; for urea formation, isocyanate coupling partner, NMM, DMF; (ii) global deprotection using TFA:H_2O:iPr_3SiH (95:2.5:2.5), followed by HPLC reverse phase purification.

dx.doi.org/10.1021/jm400416u | *J. Med. Chem.* 2013, 56, 5079−5093

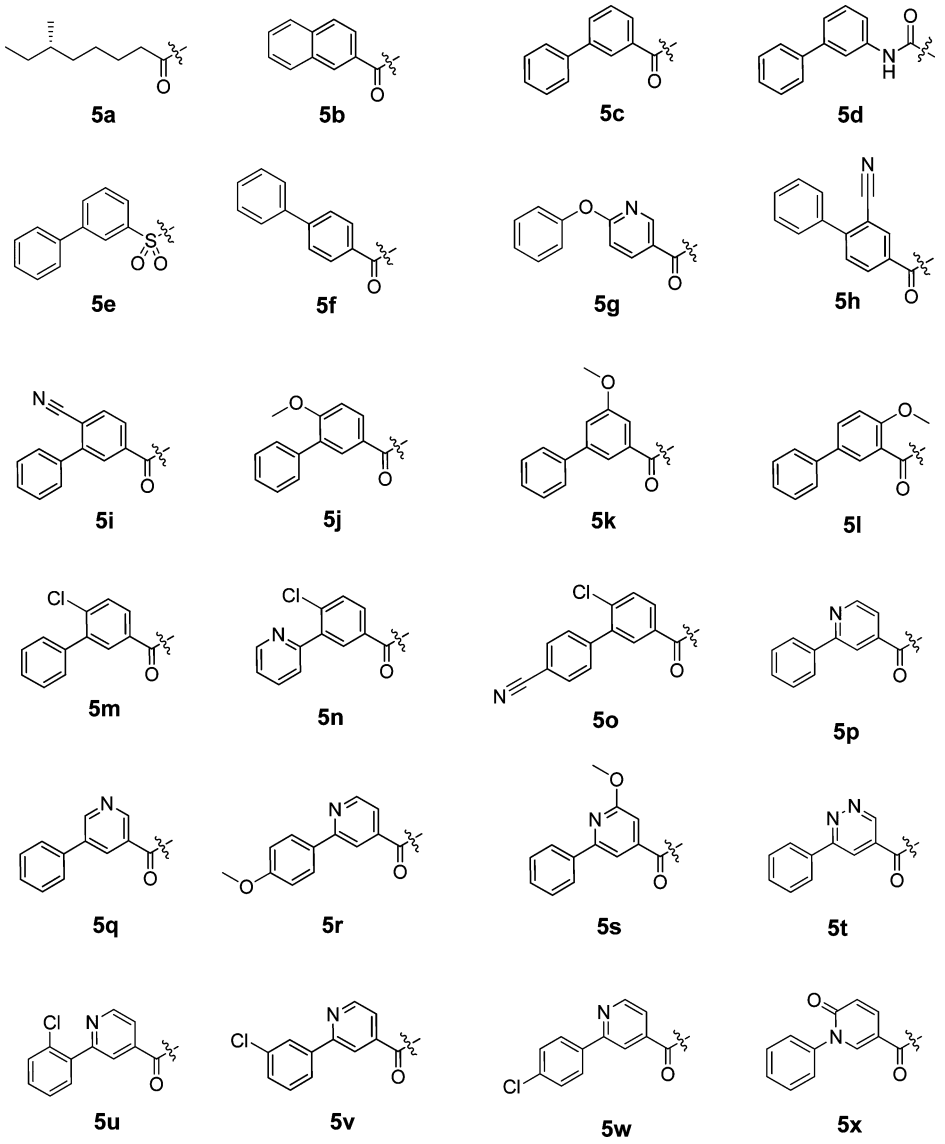

Figure 2. N-Termini (**R**) on template **5** (see Scheme 1) resulting in final analogues **5a**–**x**.

Starting with Fmoc-protected Leu attachment to the resin and standard coupling/deprotection methodology, a linear chain was constructed sequentially. With our focus on polymyxin B analogues, the D-Phe unit was first coupled to the N-terminus of the Leu-CTC resin. The L-2,4-diaminobutyric acid (Dab) residue with Boc protection on the 4-amino group was then added, followed by a Dab with 1-(4,4-dimethyl-2,6-dioxocyclohexylidene)-ethyl (Dde) on its 4-amino position. The next residue was, significantly, not the Dab traditionally found in polymyxins at this position but the L-2,3-diaminopropanoic acid (Dap) variant (3-amino Boc protected). The implications of this change will be discussed in the next section. The Thr (OtBu) and Dab (4-amino Boc) were subsequently coupled, and the N-terminus finally capped with benzyloxycarbonyl (*Z*) to yield **3**. The Dde was then selectively removed with hydrazine and the 4-amino group of this Dab unit extended sequentially, as above with Thr (OtBu) and two Dab (Boc) residues. The peptide was then cleaved off the resin with dilute TFA in DCM and subsequently cyclized in 70% yield (0.002M, EDC-HCl). Hydrogenolysis of the *Z* group gave the key intermediate **4**, which was then used for N-terminal modification using standard coupling procedures (with emphasis on amidation), followed by global deprotection with TFA, to give analogues **5a**–**x** (Figure 2).

RESULTS AND DISCUSSION

One of our first observations in this effort was that PMB was already very potent against the key pathogens of interest, namely *P. aeruginosa*, *A. baumannii*, *K. pneumoniae*, and *E. coli*. To differentiate analogues, we needed to include resistant strains in our primary screening cascade. Furthermore, we observed that the standard method of screening antibacterial potency for these resistant isolates, namely minimum inhibitory concentration (MIC), was inadequate for distinguishing between compounds and found that minimum bactericidal concentration (MBC) greatly augmented SAR interpretation by providing a broader dynamic range, in particular for *P. aeruginosa*. Thus we included, in addition to more common sensitive strains we had on hand, recent clinical isolates with a polymyxin resistant (MIC $\geq$ 8 mg/L) phenotype for the nonfermenters *P. aeruginosa* (PA-1646)[18] and *A. baumannii* (AB-1649) and ran MBC as well as MIC tests (Table 1). Our

dx.doi.org/10.1021/jm400416u | *J. Med. Chem.* 2013, 56, 5079–5093

Table 1. Minimum Bactericidal Concentrations (MBC, mg/L) and Minimum Inhibitory Concentrations (MIC, mg/L) against Polymyxin Resistant and Sensitive Strains of *P. aeruginosa* (PA), *A. baumannii* (AB), *K. pneumoniae* (KP), and *E. coli* (EC)

compd	PA-1646 MBC	PA-1646 MIC	PA-01 MIC	AB-1649 MBC	AB-1649 MIC	AB-3167 MIC	KP-3700 MIC	EC-1 MIC	hRPTEC[a] TC_{50} (μM)	cLogD	ΔcLogD[b]
PMB	32	8	0.5	8	8	0.25	0.25	0.125	22	−9.21	0
PMBN	>64	>64	>64	>64	>64	>64	>64	>64	>100	−10.69	−1.48
1	16	4	0.5	4	4	0.25	0.5	0.125	27	−9.21	0
5a	2	1	0.5	4	4	0.125	0.125	0.125	72	−9.30	−0.09
5b	16	4	0.5	2	2	0.25	0.125	0.125	51	−9.70	−0.49
5c	2	1	0.5	2	2	0.25	0.5	0.25	21	−8.53	0.68
5d	1	1	0.5	4	4	0.25	0.25	0.25	15	−9.53	−0.32
5e	4	2	0.25	>64	64	1	0.5	0.25	42	−7.90	1.31
5f	1	0.5	0.5	1	1	0.25	0.25	0.25	28	−8.75	0.46
5g	16	4	1	4	2	0.25	0.25	0.25	61	−10.13	−0.92
5h	4	2	1	1	1	0.25	0.5	0.5	32	−8.89	0.32
5i	4	2	0.25	0.5	0.5	0.25	0.25	0.125	39	−8.53	0.68
5j	2	1	0.5	2	2	0.5	0.25	0.25	27	−8.73	0.48
5k	4	2	0.5	8	4	0.25	0.25	0.25	26	−8.64	0.57
5l	2	2	0.5	4	4	0.25	0.25	0.5	19	−8.99	0.22
5m	1	0.5	1	1	1	0.5	0.25	0.25	14	−8.23	0.98
5n	16	4	1	4	4	0.25	0.25	0.25	72	−9.41	−0.2
5o	4	1	1	4	4	0.5	0.5	0.5	20	−8.91	0.3
5p	4	2	0.25	1	1	0.25	0.25	0.125	82	−9.13	0.08
5q	4	2	0.5	4	4	0.25	0.25	0.125	56	−9.42	−0.21
5r	8	2	0.5	2	2	0.25	0.25	0.25	78	−9.31	−0.1
5s	1	1	0.5	4	4	0.5	0.25	0.25	24	−8.49	0.72
5t	8	2	0.25	4	2	0.25	0.125	0.125	84	−9.76	−0.55
5u	16	4	0.5	1	1	0.25	0.25	0.125	86	−9.06	0.15
5v	1	1	0.5	0.5	0.5	0.25	0.5	0.125	34	−8.74	0.47
5w	1	1	0.5	1	1	0.25	0.25	0.25	30	−8.66	0.55
5x	8	4	0.5	2	2	0.25	0.25	0.125	>100	−11.96	−2.75

[a]Human renal proximal tubule epithelial cell line toxic concentration 50%. [b]cLogD − $cLogD_{PMB}$.

primary goal was to differentiate from the standard-of-care polymyxins against the nonfermenter (*P. aeruginosa*, *A. baumannii*) rather than the enteric strains (*K. pneumoniae*, *E. coli*). In addition to having this potency screening strategy described above, we included a high-throughput in vitro screen for gauging renal toxicity potential, as demonstrated potency advantages would be of very little interest if the renal liabilities increased correspondingly. Attempting to separate the antimicrobial potency from nephrotoxicity by achieving the right balance of physical properties remains the key challenge to improving on the polymyxin class. The multibasic polymyxins accumulate in the kidney, resulting in acute tubular necrosis, a dose-limiting toxicity. This limitation consequently impacts the therapeutic utility of the polymyxins as well as raises the specter of incomplete pathogen eradication and greater potential for the spread resistant strains. In vivo screening for improved renal toxicity profiles with preclinical animal models is not practical in discovery research mode, and while the rabbit brush border membrane assay has been cited as useful for potentiator-mode polymyxins with fewer basic amines,[11] the dynamic range of this assay was found to be insufficient for our purposes. In place of this, we utilized primary human renal proximal tubule epithelial cells (hRPTEC)[19] for in vitro kidney toxicity screening, with lactate dehydrogenase release as a cell viability end point. We were thus able to generate cytotoxicity concentration curves, and from this estimate the concentration at 50% cell viability for each analogue (TC_{50}). As of this writing, the translatability of this assay to human or preclinical species renal toxicity is not clear, however, it served as a useful guide for avoiding excessively cytotoxic analogues in human primary cells from a known target organ and for making decisions on which analogues to progress into in vivo studies. Prescription grade PMB, a fermentation mixture, was used as a reference for all assays. We observed that the MBC of PMB was 4-fold higher than the MIC (32 vs 8 mg/L) against the polymyxin resistant *P. aeruginosa* strain (PA-1646). The resistant *A. baumannii* strain (AB-1649) did not demonstrate this MBC/MIC shift, both being 8 mg/L. As expected, PMB was very potent (MICs $\leq$ 1 mg/L) against strains identified as susceptible in our screening panel (PA-01, AB-3167, KP-3700, and EC-1). Because PMB is a fermentation product and as such a mixture of components, we synthesized the major constituent (**1**) and demonstrated dilution shift in potency versus the resistant strains PA-1646 and AB-1649. The hRPTEC TC_{50} values for both PMB and **1** were generally $\leq$30 μM, which we used as a point of reference for novel analogues. PMBN, which has little or no intrinsic antimicrobial activity, had a TC_{50} > 100 μM in this assay as expected. We then set out to modulate the basicity of the polymyxin peptide template, to eliminate cationic charge if possible, or to lower the pK_a of the Dab residues. In so doing, we found that a very simple change, namely replacing the 2,4-diaminobutyric acid at position-3 of the peptide (Dab-3) with a 2,3-diaminoproprionic acid (Dap-3) residue (amounting to a single methylene excision), yielded an interesting and useful result in compound **5a** in which the antimicrobial potency improved significantly while simultaneously decreasing the hRPTEC cytotoxicity by well over 2-fold. Improving activity by shortening the Dab residue was

dx.doi.org/10.1021/jm400416u | J. Med. Chem. 2013, 56, 5079−5093

contrary to expectation[9] and worked only at the 3-position with the Dap residue. NMR studies[7b] have suggested that Dab-3 was not directly interacting with the lipid A disaccharide but rather may be involved in KDO contacts. Lack of detailed structural knowledge of how these molecules interact with LPS and affect the outer and inner membranes in living, dynamic bacteria makes speculation about the nature of our SAR difficult. The multifactorial components of what constitutes polymyxin whole cell potency do suggest that differential flexibilities within different parts of the molecule are important and that the insertion of the side chain into membranes plays a crucial role.[20] Removing degrees of freedom at the Dab-3 position, by removing a methylene in the residue side chain and bringing the charged amine closer to the backbone, might also influence the orientation or dynamics of insertion in situ. The distinct lack of rigidity in the fatty acyl portion of the side chain marked this as a further point of potential SAR and toxicity modulation. Continuing on in the Dap-3 series, replacement of the fatty acyl with a 2-napthyl acyl side chain yielded a compound (**5b**) which was less potent against PA-1646 but was a dilution better against AB-1649. The more extended (nonfused) biphenyl amide **5c** was consistently potent against both PA and AB-resistant strains, however, the cytotoxicity was comparable to PMB. Different linkers such as urea (**5d**) or sulfonyl (**5e**) yielded very mixed results, the sulfonyl in particular demonstrating a dramatic loss in AB-1649 activity. The more extended *p*-biphenyl amide **5f** appeared to have a slight potency advantage, at least for the simple case relative to the *m*-biphenyl **5c**. Heteroatom substitutions were then explored in order to test the limits of lipophilicity requirements and SAR tolerance for such changes and to monitor how polarity impacted hRPTEC cytotoxicity. Installation of more polar functional groups such as the *O*-phenylpyridone **5g**, with heteroatoms bridging the biaryl systems, generally lost activity and required us to tread somewhat carefully. Nitrile functionality in the proximal biphenyl (**5h**, **5i**) held on to potency but showed no cytotoxicity advantage. A methoxy scan (**5j**, **5k**, and **5l**) of the proximal ring of the *m*-biphenyl system was much the same, only AB-1649 dropping off with this substituent. The *m*-biaryl amides appeared to tolerate substituents (nitrile, methoxy, halogen) or heteroatom replacements best at the *p*-position of the proximal ring (viz. **5i**, **5j**, **5m**, and **5p**). The potency difference between analogues **5m** and **5n**, and even **5o**, again highlights the general intolerance for heteroatoms in the distal rings of these biaryl systems. Moving the nitrogen from the *p*-position of the proximal ring proved unproductive (**5p** vs **5q**), as were heteroatom substituents in the distal ring (e.g., **5r**). Pyridone **5s** showed improved *P. aeruginosa* activity relative to **5p**, however, the AB-1649 activity was lower and the hRPTEC cytotoxicity increased significantly. Pyridazine **5t** had a cytotoxicity profile similar to **5p** but lost potency against both PA-1646 and AB-1649, consistent with the activity loss observed in **5q**. Chloro substitution in the distal ring of **5p** yielded **5u**, **5v**, and **5w**, the latter two analogues displaying superb potency profiles although cytotoxicities within the range of PMB, and therefore not necessarily representing improvements in overall properties. Because measured Log *D* values were difficult to obtain with these extremely polar molecules we utilized calculated Log *D* values (cLogD) and in particular the difference between analogue cLogDs and that of PMB (labeled ΔcLogD, Table 1) for purposes of comparison. There was a general trend of compounds with more polar side chains (i.e., more negative ΔcLogD) having higher hRPTEC TC_{50} values relative to PMB (**5b**, **5g**, **5m**, **5q**, **5r**, **5t**), however, there were several examples where the ΔcLogD values calculated out to be more or less isolipophilic (**5a**, **5p**, **5u**) or even more lipophilic (**5e**) and still showed a higher TC_{50} outside of the standard deviations observed.[21] At this stage, we sought to make a more radical structural change in the side chain to even further reduce the hRPTEC cytotoxicity liability while maintaining or perhaps improving on our potency relative to PMB so as to test the utility of our toxicity assay for screening analogues preclinically. We capitalized on the observation that the *p*-position of the proximal aromatic ring tolerated polarity reasonably well and that chloride substitution at this position yielded extremely potent compound, albeit a cytotoxic one (**5m**). We reasoned that an *N*-phenyl pyridone (**5x**) might introduce significant polarity into the side chain without entirely losing potency. Indeed, in vitro microbiological potencies of **5x**, in particular the MBCs verus PA-1646 and AB-1649, were found to still demonstrate a slight advantage when compared to PMB. Consistent with these results were the MIC_{50} and MIC_{90} values of **5x** and PMB against larger subpopulations of *P. aeruginosa* and *A. baumannii* (Table 2). In addition, in vitro nephrotoxicity as measured by the hRPTEC assay indicated a significantly lower cytotoxicity liability of **5x** relative to PMB or any of the other analogues.[22] Notice for **5x** the ΔcLogD = −2.75 represented the largest increase in (calculated) polarity in comparison to the other analogues, with the pyridone dipole making the obvious difference as planned. A scatter plot of the hRPTEC data and ΔcLogD values shows a general trend toward lower cytotoxicity liability with increasingly negative ΔcLogD, **5x** being clearly different in both respects from PMB (Figure 3). Taken together, these data supported in vivo profiling to determine if **5x** represented the therapeutic advantage over PMB that we sought. We then moved into extensive comparative in vivo safety studies in rat and dog. A 7-day exploratory toxicology study (ETS) in rat demonstrated differentiation in the incidence of necrotic kidney lesions (Table 3). At a free exposure of 13 mg·h/L per day, **5x** exhibited no incidence of necrotic kidney lesions, whereas at a matched free exposure PMB produced necrotic kidney lesions in every animal in the dose group, albeit graded to be minimal.[23] Attempts to dose PMB at the top dose (8 mg/kg·d) failed owing to severe tolerability issues, whereas **5x** was well-tolerated and furthermore yielded no lesions, reaching a *f*AUC = 29 mg·h/L. Encouraged by these results and apparent safety differentiation observed in the rat, we then ran 7-day ETS studies in dog. The dog proved to be a more sensitive species, for although the low dose (*f*AUC = 20 mg·h/L) of **5x** was well tolerated and produced minimal nephrotoxicity, the middle dose (*f*AUC = 64 mg·h/L) and high dose (*f*AUC = 114 mg·h/

Table 2. MIC_{50} and MIC_{90} Values of 5x Compared with PMB versus Susceptible and Resistant Subpopulations of *P. aeruginosa*, *A. baumannii*, *E. coli*, and *K. pneumoniae*

	5x		PMB	
strain subgroup (*n* = number of strains)	MIC_{50}	MIC_{90}	MIC_{50}	MIC_{90}
susceptible *P. aeruginosa* (*n* = 96)	1	2	2	2
susceptible *A. baumannii* (*n* = 96)	2	2	2	2
susceptible *E. coli* (*n* = 101)	1	2	1	2
susceptible *K. pneumoniae* (*n* = 100)	0.5	1	1	2
resistant *P. aeruginosa* (*n* = 6)	2	8	4	16
resistant *A. baumannii* (*n* = 17)	4	16	16	>64

dx.doi.org/10.1021/jm400416u | *J. Med. Chem.* 2013, 56, 5079−5093

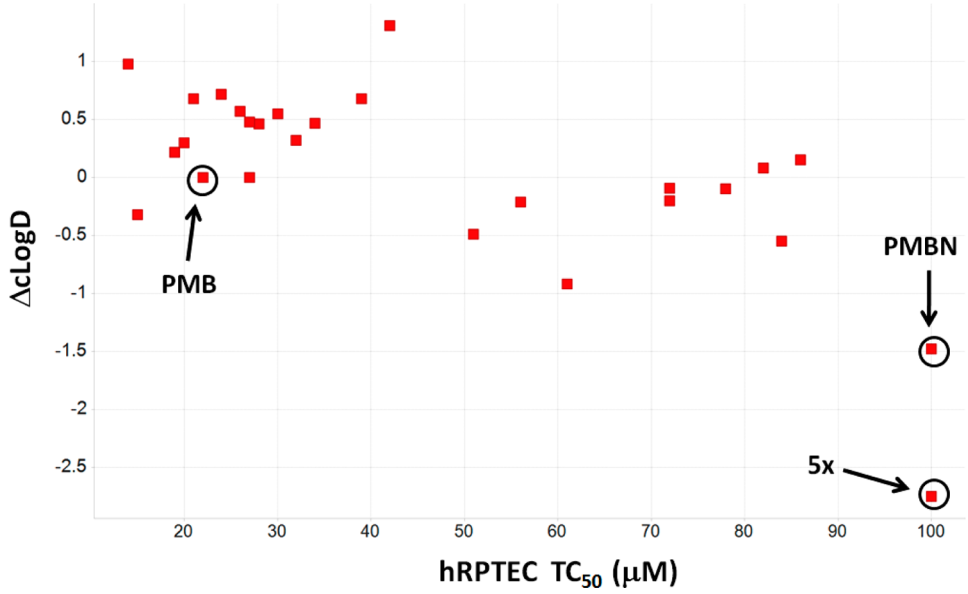

Figure 3. Scatter plot of hRPTEC TC_{50} data and ΔcLogD highlighting PMB and **5x**. Note that the TC_{50} > 100 μM for **5x** (and PMBN) in this assay, however, they are indicated as equal to 100 μM on this plot for purposes of illustration.

Table 3. Rat (7d) and Dog (7d) Exploratory Toxicology Study (ETS) Results of 5x and PMB

5x				PMB			
dose[a] (mg/kg·d)	*f*AUC[b] (mg·h/L)	*N*[c]	histological assessment[d]	dose[a] (mg/kg·d)	*f*AUC[e] (mg·h/L)	*N*[c]	histological assessment[d]
			Rat				
low dose not examined	low dose not examined	low dose not examined	low dose not examined	0.4	0.72	3	0/3
4	13	3	0/3	4	13	3	3/3 all minimal
8	29	3	0/3	8	high dose not tolerated	high dose not tolerated	high dose not tolerated
			Dog				
5	20	8	8/8 all minimal	1	10	2	0/2
11	64	8	8/8	6	42	8	8/8
			5 moderate				2 moderate
			3 marked				6 marked
20	114	2	2/2 all marked	high dose not examined	high dose not examined	high dose not examined	high dose not examined

[a]Doses given BID (Q12) intravenously. [b]Free AUC per day for **5x**: plasma f_u in rat and dog = 0.81 and 0.58, respectively. [c]Number of animals tested per dose group. [d]Kidney proximal tubules were evaluated for the presence of tubular epithelial degeneration/regeneration, and the resulting assessments were graded in severity from none to marked; the number of animals in which lesions appeared out of the total number tested are indicated as a ratio. [e]Free AUC per day for PMB: plasma f_u in rat and dog = 0.30 and 0.35, respectively.

L) both produced moderate or marked lesions in every animal. The PMB mid dose was targeted to mimic a *f*AUC in human for an efficacious exposure level and powered with eight animals to compare to **5x** at its mid dose. Although there were differences in the severity of the lesions slightly in favor of **5x**, and although the *f*AUC of **5x** was approximately 1.5-fold higher than PMB (64 vs 42 mg·h/L) at this dose, we deemed that there was no significant safety margin in favor of **5x** as measured by this study, at least in the dog. This result demonstrates that the substantial in vitro differentiation observed in the hRPTEC assay for **5x** versus PMB did not translate in definitive dog in vivo safety studies. Ideally, in vitro−in vivo correlations would be investigated with cells derived from the same species. Therefore, further work on species-specific in vitro assays that predict for the sensitive (nonrodent) renal toxicities in preclinical models may be warranted for selection and progression of novel polymyxin analogues to the clinic. However, we also profiled **5x** and PMB in a murine neutropenic thigh infection model[24] against composited strains of *P. aeruginosa* and observed that the PK/PD of **5x**, when matched for *f*AUC/MIC relative to PMB, did not perform as well as the latter (Table 4). The resulting pharmacokinetics of **5x** and PMB were best described using a one-compartment model with first-order input and elimination. During bacterial density studies, doses of **5x** and PMB resulted in *f*AUCs (mg·h/L) ranging from 7.2 to 775 and 18 to 51, respectively. The average bacterial densities at the start of therapy were 5.37 ± 0.12 $\log_{10}$CFU and increased to 8.85 ± 0.28 $\log_{10}$CFU after 24 h in untreated control animals. The R^2 value for the respective E_{max} models was 0.83 for **5x** and 0.97 for PMB. The pharmacodynamic direct comparison, i.e., the *f*AUC/MIC values required for similar efficacy targets, was

dx.doi.org/10.1021/jm400416u | *J. Med. Chem.* 2013, 56, 5079−5093

Table 4. Comparative Pharmacodynamics of 5x and PMB against a Composited Data Set of *P. aeruginosa* 1401 and 1402 (MICs = 0.5 mg/L) in the Neutropenic Thigh Infection Model

	*f*AUC/MIC	
efficacy parameter	**5x**	PMB
EI_{80}[a]	157.55	59.00
EI_{50}[a]	87.92	37.38
stasis	85.26	37.07
1 Log decrease	109.63	44.95

[a]Exposure index required for 80% (EI_{80}) and 50% (EI_{50}) of maximal efficacy.

greater for **5x** on all four efficacy parameters (EI_{80}, EI_{50}, Stasis, and 1 Log decrease) as compared with PMB.

CONCLUSION

We have made structural modifications to the polymyxin lipopeptide, in particular replacing the Dab with the truncated Dap residue at position-3 in the exocyclic peptide region.[25] It was surprising that such a subtle change would affect the potency as dramatically as it did. We were also able to replace the fatty acid side chain with a variety of biaryl amides which, when combined with the Dap-3 modification, led to further potency improvements, in particular against *P. aeruginosa* and *A. baumannii* resistant strains. Our primary goal was to improve the therapeutic index with a novel polymyxin analogue by reducing the nephrotoxicity liability, and to that end we utilized an in vitro human cell line for estimating the risk of renal cytotoxicity (hRPTEC). We observed that a combination of the Dap-3 substitution and a pyridone-biaryl amide (**5x**) provided a significantly different signature in hRPTEC without compromising potency. Exploratory toxicity studies (ETS) suggested that **5x** was better tolerated in rat with respect to renal lesions, however, this advantage collapsed in the dog, pointing to the failure of the hRPTEC assay to predict for that species. The human translatability of these safety data is not clear, however, this provides a significant barrier to further development. Furthermore, **5x** proved to be inferior in the direct PK/PD comparison with PMB in the murine neutropenic thigh model, suggesting that the overall therapeutic index of this analogue is not likely to surpass that of PMB and highlighting the importance of conducting rigorous, free exposure matched efficacy comparisons when making changes to the polymyxin structure.

EXPERIMENTAL SECTION

All final peptide analogues were isolated by preparative HPLC to ≥98% purity and analyzed by high resolution mass spectrometry. Pharmaceutical grade PMB (Bedford Laboratories) was used in all experiments. MS data were collected on an Agilent (Wilmington, DE) 6220 Accurate Mass TOF LC/MS operating in the electrospray ionization mode. The chromatography system consisted of an Agilent (Wilmington, DE, USA) 1200 binary pumping system with the addition of an extra isocratic system and a dynamic splitter for dilution of samples as they passed between the UV detector and the mass spectrometer. The binary pump operated at 1.1 mL/min of A = 10 mM ammonium formate adjusted to pH 3.5 in water and B = 50:50 acetonitrile:methanol. Sample injections were typically 0.5 μL. Separations were effected using an Agilent Zorbax Eclipse Plus C-18 (3.0 mm × 50 mm, 1.8 μm) column operating at 60 °C. As samples eluted the UV detector, they were diluted in the dynamic splitter with an isocratic pump flowing at 0.5 mL/min and using a solvent of 50:50 MeOH:water. Samples were diluted by factors ranging from 33:1 to 100:1. Data was processed using the MassHunter software that was provided with the instrument. All test peptides were analyzed using a Bruker 500 MHz spectrometer. Small molecule intermediates were analyzed with a Varian Inova 400 MHz spectrometer.

Synthesis of Protected Template 5: H-Dab(Boc)-Thr(tBu)-Dap(Boc)-cyclo[Dab-Dab(Boc)-DPhe-Leu-Dab(Boc)-Dab(Boc)-Thr(tBu)]. *Step 1: Fmoc-Leu-CTC Resin.* CTC resin (950g, 988 mmol) was suspended in DCM (8L) in a peptide synthesis vessel equipped with a mechanical stirrer. To the suspension was added Fmoc-Leu-OH (349 g, 988 mmol) and DIPEA (863 mL, 4940 mmol). The mixture was stirred gently at RT for 3h. To the reaction was added 0.95 L of MeOH. The resulting mixture was stirred at RT for 0.5 h and then filtered. Solid was washed with DCM (3 × 15L) and subsequently MeOH (2 × 10L). The resulting solid was dried under vacuum overnight to furnish 1250 g of Fmoc-Leu-CTC resin.

The loading level of the resin product thus obtained was established to be 0.46 mmol/g via standard UV absorption method (Shimadzu UV-1601, wavelength 289.5 nm) upon Fmoc cleavage of small aliquots of the product resin.

Step 2: Fmoc-DPhe-Leu-CTC Resin. Fmoc-Leu-CTC resin (152g, 0.46 mmol/g, 70 mmol) was suspended in DMF (1 L) at RT overnight in a peptide synthesis vessel equipped with a mechanical stirrer. DMF was then removed via filtration. To the solid was added 20% piperidine in DMF (1.0 L), and the resulting mixture was stirred at 18 °C for 0.5 h. Mixture was then filtered. Solid resin H-Leu-CTC was washed with DMF (6 × 1 L).

Fmoc-DPhe-OH (54.2g, 140 mmol) and HOBt (18.9g, 140 mmol) were dissolved in DMF (0.25L) at 0 °C. To the mixture was added DIC (22.1 mL, 140 mmol) at 0 °C in one portion, and mixture was kept at 0 °C for 15 min. The activated AA solution was then added into the H-Leu-CTC resin, and the mixture was stirred at 18 °C for 1 h, at which point Kaiser ninhydrin test indicated reaction completion. The mixture was filtered and solid was washed with DMF (5 × 1 L). The Fmoc-DPhe-Leu-CTC resin product was used in the subsequent step without further treatment.

Step 3: Fmoc-Dab(Boc)-DPhe-Leu-CTC Resin. To the Fmoc-DPhe-Leu-CTC resin in a peptide synthesis vessel equipped with a mechanical stirrer, obtained from step 2, was added 20% piperidine in DMF (1 L), and the resulting mixture was stirred gently at 20 °C for 0.5 h. The mixture was then filtered. Solid resin H-DPhe-Leu-CTC was washed with DMF (6 × 1 L).

Fmoc-Dab(Boc)-OH (61.6g, 140 mmol) and HOBt (18.9 g, 140 mmol) were dissolved in DMF (0.25 L) at 0 °C. To the mixture was added DIC (22.1 mL, 140 mmol) at 0 °C in one portion, and the mixture was kept at 0 °C for 15 min. The activated AA solution was then added into H-DPhe-Leu-CTC resin, and the mixture was stirred at 19 °C for 1 h, at which point Kaiser ninhydrin test indicated reaction completion. The mixture was filtered and solid was washed with DMF (5 × 1 L). The resulting Fmoc-Dab(Boc)-DPhe-Leu-CTC resin product was used in the subsequent step without further treatment.

Step 4: Fmoc-Dab(Dde)-Dab(Boc)-DPhe-Leu-CTC Resin. To the Fmoc-Dab(Boc)-DPhe-Leu-CTC resin in a peptide synthesis vessel equipped with a mechanical stirrer, obtained from step 3, was added 20% piperidine in DMF (1 L), and the resulting mixture was stirred at 19 °C for 0.5 h. The mixture was then filtered. Solid H-Dab(Boc)-DPhe-Leu-CTC resin was washed with DMF (6 × 1 L).

Fmoc-Dab(Dde)-OH (70.4 g, 140 mmol) and HOBt (18.9g, 140 mmol) were dissolved in DMF (0.25L) at 0 °C. To the mixture was added DIC (22.1 mL, 140 mmol) at 0 °C in one portion, and the mixture was kept at 0 °C for 15 min. The activated AA solution was then added into H-Dab(Boc)-DPhe-Leu-CTC resin, and the mixture was stirred at 21 °C for 1 h, at which point Kaiser ninhydrin test indicated reaction completion. The mixture was filtered and solid was washed with DMF (5 × 1 L). The resulting Fmoc-Dab(Dde)-Dab(Boc)-DPhe-Leu-CTC resin product was used in subsequent step without further treatment.

Step 5: Fmoc-Dap(Boc)-Dab(Dde)-Dab(Boc)-DPhe-Leu-CTC Resin. To the resin Fmoc-Dab(Dde)-Dab(Boc)-DPhe-Leu-CTC in a

dx.doi.org/10.1021/jm400416u | J. Med. Chem. 2013, 56, 5079−5093

peptide synthesis vessel equipped with a mechanical stirrer, obtained from the step 4, was added 20% piperidine in DMF (1.5 L), and the resulting mixture was stirred at 22 °C for 0.5 h. Mixture was then filtered. Solid H-Dab(Dde)-Dab(Boc)-DPhe-Leu-CTC resin was washed with DMF (6 × 1.5 L).

Fmoc-Dap(Boc)-OH (59.6 g, 140 mmol) and HOBt (18.9g, 140 mmol) were dissolved in DMF (0.25 L) at 0 °C. To the mixture was added DIC (22.1 mL, 140 mmol) at 0 °C in one portion, and the mixture was kept at 0 °C for 15 min. The activated AA solution was then added into H-Dab(Dde)-Dab(Boc)-DPhe-Leu-CTC resin, and mixture was stirred at 22 °C for 1 h, at which point the Kaiser ninhydrin test indicated reaction completion. The mixture was filtered and the solid was washed with DMF (5 × 1 L). The resulting Fmoc-Dap(Boc)-Dab(Dde)-Dab(Boc)-DPhe-Leu-CTC resin product was confirmed by peptide cleavage and subsequent HPLC and LCMS analysis outlined below.

A small portion of the resin product (1 mL) was washed with MeOH (3 × 5 mL) and then dried overnight under vacuum. The resin was then treated with 5 mL of solution F at RT for 2.5 h. The reaction mixture was filtered, and the filtrate was quenched with cold ether (50 mL). A white solid formed, and this solid was collected via removal of the solvent after the mixture was centrifuged. The solid residue was washed with cold ether (2 × 50 mL), dried under vacuum overnight, and analyzed using an HP1090 system connected to a SepaxGP-C18 (5 μm, 120A, 4.6 mm × 150 mm) reversed-phase HPLC column. Gradient method: 15−75% solvent B over 20 min at a flow rate of 1.0 mL/min (solvent A,: 0.1% TFA in water; solvent B, 0.09% TFA, 20% water, and 79.91% eMeCN). Major peak with retention time 13.8 min, 78.1% by UV220; ESI-MS (Thermo LCQ advantage): (m/z) = 951.4 ($[M + H]^+$), 476.4 ($[M + 2H]^{2+}/2$).

Step 6: Fmoc-Thr(tBu)-Dap(Boc)-Dab(Dde)-Dab(Boc)-DPhe-Leu-CTC Resin. To the resin Fmoc-Dap(Boc)-Dab(Dde)-Dab(Boc)-DPhe-Leu-CTC in a peptide synthesis vessel equipped with a mechanical stirrer, obtained from step 5, was added 20% piperidine in DMF (1.5 L), and the resulting mixture was stirred kept at 21 °C for 0.5 h. The mixture was then filtered. The solid H-Dap(Boc)-Dab(Dde)-Dab-(Boc)-DPhe-Leu-CTC resin was washed with DMF (6 × 1.5 L).

Fmoc-Thr(tBu)-OH (55.6g, 140 mmol) and HOBt (18.9g, 140 mmol) were dissolved in DMF (0.25L) at 0 °C. To the mixture was added DIC (22.1 mL, 140 mmol) at 0 °C in one portion, and the mixture was kept at 0 °C for 15 min. The activated AA solution was then added into H-Dap(Boc)-Dab(Dde)-Dab(Boc)-DPhe-Leu-CTC resin, and the mixture was stirred for 1 h, at which point the Kaiser ninhydrin test indicated reaction completion. The mixture was filtered and the solid was washed with DMF (5 × 1L). The resulting Fmoc-Thr(tBu)-Dap(Boc)-Dab(Dde)-Dab(Boc)-DPhe-Leu-CTC resin product was confirmed by peptide cleavage and subsequent HPLC and LCMS analysis outlined in step 5.

Gradient method: 15−75% solvent B over 20 min at a flow rate of 1.0 mL/min (solvent A, 0.1% TFA in water; solvent B, 0.09% TFA, 20% water, and 79.91% MeCN). Major peak with retention time 19.3 min, 89.6% by UV220; ESI-MS (Thermo LCQ advantage): (m/z) = 1052.5 ($[M + H]^+$), 527.0 ($[M + 2H]^+/2$).

Step 7: Fmoc-Dab(Boc)-Thr(tBu)-Dap(Boc)-Dab(Dde)-Dab(Boc)-DPhe-Leu-CTC Resin. To the resin Fmoc-Thr(tBu)-Dap(Boc)-Dab-(Dde)-DPhe-Leu-CTC in a peptide synthesis vessel equipped with a mechanical stirrer, obtained from step 6, was added 20% piperidine in DMF (1.5 L), and the resulting mixture was stirred at 21 °C for 0.5 h. The mixture was then filtered and the resin H-Thr(tBu)-Dap(Boc)-Dab(Dde)-Dab(Boc)-DPhe Leu-CTC was washed with DMF (6 × 1.5 L).

Fmoc-Dab(Boc)-OH (61.6 g, 140 mmol) and HOBt (18.9g, 140 mmol) were dissolved in DMF (0.25 L) at 0 °C. To the mixture was added DIC (22.1 mL, 140 mmol) at 0 °C in one portion, and the mixture was kept at 0 °C for 15 min. The activated AA solution was then added into H-Thr(tBu)-Dap(Boc)-Dab(Dde)-Dab(Boc)-DPhe-Leu-CTC resin, and the mixture was stirred at 22 °C for 1 h, at which point the Kaiser ninhydrin test indicated reaction completion. The mixture was filtered and the solid was washed with DMF (5 × 1 L). The Fmoc-Dab(Boc)-Thr(tBu)-Dap(Boc)-Dab(Dde)-Dab(Boc)-DPhe-Leu-CTC resin product was confirmed by peptide cleavage and subsequent HPLC and LCMS analysis outlined in step 5.

Gradient method: 15−75% solvent B over 20 min at a flow rate of 1.0 mL/min (solvent A, 0.1% TFA in water; solvent B, 0.09% TFA, 20% water, and 79.91% MeCN). Major peak with retention time 17.5 min, 78.7% by UV220; ESI-MS (Thermo LCQ advantage): (m/z) = 1152.5 ($[M + H]^+$), 577.9 ($[M + 2H]^+/2$).

Step 8: Z-Dab(Boc)-Thr(tBu)-Dap(Boc)-Dab(Dde)-Dab(Boc)-DPhe-Leu-CTC Resin. To the resin Fmoc-Dab(Boc)-Thr(tBu)-Dap-(Boc)-Dab(Dde)-DPhe-Leu-CTC in a peptide synthesis vessel equipped with a mechanical stirrer, obtained from the step 7, was added into 20% piperidine in DMF (2.0 L), and the resulting mixture was stirred at RT for 0.5 h. The mixture was then filtered, and the solid H-Dab(Boc)-Thr(tBu)-Dap(Boc)-Dab(Dde)- Dab(Boc)-DPhe-Leu-CTC resin was washed with DMF (5 × 2L). To the resin was then added a solution of Z-OSu (52.3g, 210 mmol) and NMM (46.2 mmol, 420 mmol) in DMF (0.50 L). The resulting mixture was stirred for 1 h. Kaiser ninhydrin test indicated reaction completion. The mixture was filtered after stirred at RT for another 50 min. Solid was washed with DMF (5 × 2 L), and the product, Z-Dab(Boc)-Thr(tBu)-Dap(Boc)- Dab(Dde)-Dab(Boc)-DPhe-Leu-CTC resin product, was confirmed by peptide cleavage and subsequent HPLC and LCMS analysis outlined in step 5.

Gradient method: 15−75% solvent B over 20 min at a flow rate of 1.0 mL/min (solvent A, 0.1% TFA in water; solvent B, 0.09% TFA, 20% water, and 79.91% MeCN). Major peak with retention time 11.7 min, 73.7% by UV220; ESI-MS (Thermo LCQ advantage): (m/z) = 1064.5 ($[M + H]^+$), 533.0 ($[M + 2H]^+/2$).

Step 9: Z-Dab(Boc)-Thr(tBu)-Dap(Boc)-Dab[Thr(tBu)-Fmoc]-Dab-(Boc)-DPhe-Leu-CTC Resin. To the resin Z-Dab(Boc)-Thr(tBu)-Dap(Boc)-Dab(Dde)-Dab(Boc)-DPhe-Leu-CTC in a peptide synthesis vessel equipped with a mechanical stirrer, obtained from step 8, was added a solution of 3% hydrazine in DMF (2L). The resulting mixture was stirred at 20 °C for 0.5h. The mixture was then filtered and the solid Z-Dab(Boc)-Thr(tBu)-Dap(Boc)-Dab[-H]- Dab(Boc)-DPhe-Leu-CTC resin was washed with DMF (5 × 2L).

Fmoc-Thr(tBu)-OH (55.6g, 140 mmol) and HOBt (18.9 g, 140 mmol) were dissolved in DMF (0.3L) at 0 °C. To the mixture was added DIC (22.1 mL, 140 mmol) at 0 °C in one portion and the mixture was kept at 0 °C for 15 min. The activated AA solution was then added into the resin Z-Dab(Boc)-Thr(tBu)-Dap(Boc)-Dab[-H]-Dab(Boc)- DPhe-Leu-CTC and the mixture was stirred at 18 °C for 1h at which point Kaiser ninhydrin test indicated reaction completion. The mixture was stirred for an additional 1h then filtered. The solid was washed with DMF (5 × 1L) and the resin product Z-Dab(Boc)-Thr(tBu)-Dap(Boc)-Dab[Thr(tBu)-Fmoc]-DPhe-Leu-CTC was confirmed by peptide cleavage and subsequent HPLC and LCMS analysis outlined in step 5.

Gradient method: 15−75% solvent B over 20 min at a flow rate of 1.0 mL/min (solvent A, 0.1% TFA in water; solvent B, 0.09% TFA, 20% water, and 79.91% MeCN). Major peak with retention time 13.8 min, 91.1% by UV220; ESI-MS (Thermo LCQ advantage): (m/z) = 1223.5 ($[M + H]^+$), 612.6 ($[M + 2H]^+/2$).

Step 10: Z-Dab(Boc)-Thr(tBu)-Dap(Boc)-Dab[Thr(tBu)-Dab(Boc)-Fmoc]-Dab(Boc)-DPhe-Leu-CTC Resin. To the resin Z-Dab(Boc)-Thr(tBu)-Dap(Boc)-Dab[Thr(tBu)-Fmoc]-Dab(Boc)-DPhe-Leu-CTC in a peptide synthesis vessel equipped with a mechanical stirrer, obtained from step 9, was added 20% piperidine in DMF (2 L), and the resulting mixture was stirred at 19 °C for 0.5 h. The mixture was then filtered, and the solid Z-Dab(Boc)-Thr(tBu)-Dap(Boc)-Dab-[Thr(tBu)-H)]-Dab(Boc)-DPhe-Leu-CTC resin was washed with DMF (5 × 2 L).

Fmoc-Dab(Boc)-OH (61.6 g, 140 mmol) and HOBt (18.9 g, 140 mmol) were dissolved in DMF (0.3 L) at 0 °C. To the mixture was added DIC (22.1 mL, 140 mmol) at 0 °C in one portion, and the mixture was kept at 0 °C for 15 min. The activated AA solution was then added into Z-Dab(Boc)-Thr(tBu)-Dap(Boc)-Dab[Thr(tBu)-H]-Dab(Boc)-DPhe-Leu-CTC, and the mixture was stirred at 19 °C for 1 h at which point the Kaiser ninhydrin test indicated reaction completion. The mixture was stirred for an additional 1 h and then

filtered. The solid was washed with DMF (5 × 2 L). The resin product Z-Dab(Boc)-Thr(tBu)-Dap(Boc)-Dab[Thr(tBu)-Dab(Boc)-Fmoc]-Dab(Boc)-DPhe-Leu-CTC was confirmed by peptide cleavage and subsequent HPLC and LCMS analysis outlined in step 5.

Gradient method: 15−75% solvent B over 20 min at a flow rate of 1.0 mL/min (solvent A, 0.1% TFA in water; solvent B, 0.09% TFA, 20% water, and 79.91% MeCN). Major peak with retention time 16.3 min, 79.2% by UV220; ESI-MS (Thermo LCQ advantage): (m/z) = 1323.5 ([M + H]$^+$), 662.5 ([M + 2H]$^+$/2).

Step 11: Z-Dab(Boc)-Thr(tBu)-Dap(Boc)-Dab[Thr(tBu)-Dab(Boc)-Dab(Boc)-Fmoc]-Dab(Boc)-DPhe-Leu-CTC Resin. To the resin Z-Dab(Boc)-Thr(tBu)-Dap(Boc)-Dab[Thr(tBu)-Dab(Boc)-Fmoc]-Dab(Boc)-DPhe-Leu-CTC in a peptide synthesis vessel equipped with a mechanical stirrer, obtained from step 10, was added 20% piperidine in DMF (2 L), and the resulting mixture was stirred at 21 °C for 0.5 h. The mixture was then filtered. Solid Z-Dab(Boc)-Thr(tBu)-Dap(Boc)-Dab[Thr(tBu)-Dab(Boc)-H)]-Dab(Boc)-DPhe-Leu-CTC resin was washed with DMF (5 × 2L).

Fmoc-Dab(Boc)-OH (61.6 g, 140 mmol) and HOBt (18.9 g, 140 mmol) were dissolved in DMF (0.3L) at 0 °C. To the mixture was added DIC (22.1 mL, 140 mmol) at 0 °C in one portion, and the mixture was kept at 0 °C for 15 min. The activated AA solution was then added into Z-Dab(Boc)-Thr(tBu)-Dap(Boc)-Dab[Thr(tBu)-Dab(Boc)-H]-Dab(Boc)-DPhe-Leu-CTC, and the mixture was stirred at 22 °C for 1 h, at which point Kaiser ninhydrin test indicated reaction completion. The mixture was stirred for 1 more hour and then filtered. The solid was washed with DMF (5 × 2L), and the Z-Dab(Boc)-Thr(tBu)-Dap(Boc)-Dab[Thr(tBu)-Dab(Boc)-Dab(Boc)-Fmoc]-Dab(Boc)-DPhe-Leu-CTC was confirmed by peptide cleavage and subsequent HPLC and LCMS analysis outlined in step 5.

Gradient method: 15−75% solvent B over 20 min at a flow rate of 1.0 mL/min (solvent A, 0.1% TFA in water; solvent B, 0.09% TFA, 20% water, and 79.91% MeCN). Major peak with retention time 14.9 min, 84.2% by UV220; ESI-MS (Thermo LCQ advantage): (m/z) = 1423.6 ([M + H]$^+$), 712.5 ([M + 2H]$^+$/2).

Step 12: Z-Dab(Boc)-Thr(tBu)-Dap(Boc)-cyclo[Dab-Dab(Boc)-DPhe-Leu-Dab(Boc)-Dab(Boc)-Thr(tBu)]. To the resin Z-Dab(Boc)-Thr(tBu)-Dap(Boc)-Dab[Thr(tBu)-Dab(Boc)-Dab(Boc)-Fmoc]-Dab(Boc)-DPhe-Leu-CTC in a peptide synthesis vessel equipped with a mechanical stirrer, obtained from step 11, was added 20% piperidine in DMF (2 L), and the resulting mixture was stirred at 23 °C for 0.5 h. The mixture was then filtered. The solid resin Z-Dab(Boc)-Thr(tBu)-Dap(Boc)-Dab[Thr(tBu)-Dab(Boc)-Dab(Boc)-H]-Dab(Boc)-DPhe-Leu-CTC was washed with DMF (5 × 2 L).

To the resin was then added 6 L of 1.5% TFA in DCM, and the resulting mixture was stirred at RT for 0.5 h. The mixture was then filtered. The filtrate was neutralized with the addition of DIPEA (approximately 180 mL) to neutral pH. The mixture was then concentrated to remove DCM. The residue was dissolved in 35 L of DMF to make up a solution of the cleaved acyclic peptide in 0.002 M concentration. To this solution was added DIPEA (61.3 mL, 350 mmol) and EDC-HCl (26.8g, 140 mmol). The resulting mixture was stirred at RT. LCMS indicated cyclization reaction completed after overnight stirring. DMF was removed on the rotary evaporator with water bath temperature no higher than 40 °C. The residue was dissolved in DCM (1.5 L), and the DCM solution was washed with water (4 × 0.7 L). DCM layer was concentrated and dried under high vacuum to furnish 130 g of the desired cyclic peptide Z-Dab(Boc)-Thr(tBu)-Dap(Boc)-cyclo[Dab-Dab(Boc)-DPhe-Leu-Dab(Boc)-Dab-(Boc)-Thr(tBu)] as a light-yellow solid.

HPLC and LCMS analysis gradient method: 70−100% B over 20 min at a flow rate of 1.0 mL/min (A, 0.1% TFA in water; B, 0.1% TFA in 80% MeCN and 20% water). Major peak with retention time 17.24 min, 70.5% by UV220; ESI-MS (Thermo LCQ advantage): (m/z) = 1795.7 ([M + H]$^+$), 898.6 ([M + 2H]$^+$/2). High resolution mass spectrometry result indicated the presence of M + 1, M + 2, M + 3 isotope distribution pattern consistent with the desired monocyclic peptide product.

Step 13: H-Dab(Boc)-Thr(tBu)-Dap(Boc)-cyclo[Dab-Dab(Boc)-DPhe-Leu-Dab(Boc)-Dab(Boc)-Thr(tBu)]. To a stirred solution of Z-Dab(Boc)-Thr(tBu)-Dap(Boc)-cyclo[Dab-Dab(Boc)-DPhe-Leu-Dab-(Boc)-Dab(Boc)-Thr(tBu)] (obtained from step 12, 130 g, assuming 70 mmol) in DCM/MeOH (1.5 L/1.5 L) in a round-bottom-flask was added concentrated ammonium hydroxide (10 mL). This mixture was then purged with N_2, and 10% Pd/C (dry, 15g) was added under nitrogen. The reaction mixture was stirred at 15 °C under 1.1 atmospheric pressure hydrogen for 4 d. The hydrogen source was removed, and the system was purged with nitrogen. The mixture was then filtered through a pad of Celite, and filtrate was concentrated in vacuum to furnish a yellow solid, 123 g (crude yield 94%).

HPLC and LCMS analysis gradient method: 70−100% solvent B over 20 min at a flow rate of 1.0 mL/min (solvent A, 0.1% TFA in water; solvent B, 0.09% TFA, 20% water, and 79.91% MeCN). Major peak with retention time 13.4 min, 78.7% by UV220; ESI-MS (Thermo LCQ advantage) (m/z) = 1662.6 ([M + H]$^+$), 831.43 ([M + 2H]$^+$/2).

Coupling and Deprotection of Template 5 to Generate Final Test Analogues. *General Procedure for Preparation of Amide Analogues:* ***5p.*** Step 1: A solution of H-Dab(Boc)-Thr(tBu)-Dap(Boc)-cyclo[Dab-Dab(Boc)-DPhe-Leu-Dab(Boc)-Dab(Boc)-Thr-(tBu)] (127 g, 76.5 mmol), 2-phenylisonicotinic acid (15.2 g, 76.5 mmol), HATU (35 g, 91.8 mmol), and NMM (25.3 mL, 230 mmol) in DMF (1700 mL) in a 3 L round-bottom flask was stirred at RT overnight. TLC indicated complete consumption of the carboxylic acid starting material (DCM/MeOH/AcOH: 40/1/0.5); MS confirmed reaction was complete. The mixture was concentrated in vacuum to remove the majority of DMF. The residue was poured into water (9 L). A white solid formed, which was collected via filtration. The filter cake was washed with water (2 L) and dried under vacuum to give 125 g of the amide intermediate as a yellow solid (89% yield), which was used in the next step without further purification.

Step 2: Into a 3 L round-bottom flask at 0 °C was charged, with the yellow solid amide intermediate from step 1 (125g, 76.8 mmol), solution F (TFA:water:iPr_3SiH 95:2.5:2.5) (1000 mL). The mixture was stirred at 0 °C for 0.5 h and RT for 2 h. The reaction mixture was quenched with cold ether (10 L), whereupon a white precipitate formed and was collected by removing the supernatant after centrifugation. This solid crude product was then purified by preparative HPLC to give the desired final amide target analogue as a white solid (TFA salt). The TFA salt thus obtained was converted to the sulfate salt by loading onto to a Novasep-C18 10 μm 100A 50 mm × 450 mm column and eluted, at a flow rate of 400 mL/min, initially with 90% A and 10% B for 3 column volumes, then 10% B and 90% C for 3 column volumes, and finally 40% B and 60% C for 1.5 column volumes (A, 0.2% H_2SO_4 in water; B, 100% MeCN; C, 100% water). The fractions containing product were combined and lyophilized to furnish 24 g of a white solid (overall yield 29%).

General Procedure for Preparation of Urea Analogues: ***5d.*** Step 1: A solution of H-Dab(Boc)-Thr(tBu)-Dap(Boc)-cyclo[Dab-Dab-(Boc)-DPhe-Leu-Dab(Boc)-Dab(Boc)-Thr(tBu)] (425 mg, 0.256 mmol), the isocyanate (50 mg, 0.256 mmol), and NMM (0.078 mL, 0.768 mmol) in DMF (10 mL) was stirred at RT for 4 h. MS indicated the reaction was complete. The mixture was concentrated in vacuum. The residue was dissolved in DCM (10 mL) and water (10 mL). The mixture was concentrated to remove DCM. White precipitate formed, and the solid was collected and dried under high vacuum to give a yellow solid (300 mg, yield 64%).

Step 2: The crude product from step 1 (300 mg, 0.162 mmol) was dissolved in solution F (TFA:water:iPr_3SiH 95:2.5:2.5) (3 mL) and stirred at RT for 2 h. The reaction mixture was quenched with cold ether (30 mL). White precipitate formed, and the solid was isolated upon removal of the supernatant after the mixture was centrifuged. The solid was then purified by preparative HPLC to give pure product (62 mg, yield 30%) as a white solid. Preparative HPLC method: crude product dissolved in MeCN/water (5/95), loaded onto a 50 mm × 250 mm 10 miron Luna C18 column and purified using a 25−50% B in 60 min at a flow rate of 60 mL/min (A, 0.1% TFA in water; B, MeCN with 0.1% TFA). Product thus obtained was 85% pure and was resubjected to preparative HPLC purification again using an isocratic 34% B method, and the desired product was obtained in >97% purity.

dx.doi.org/10.1021/jm400416u | J. Med. Chem. 2013, 56, 5079−5093

Analytical method: 32% B to 42% B in 20 min at a flow rate of 1.0 mL/min on a SepaxGP-C18, 3 μm, 120 A, 4.6 mm × 150 mm column using UV 220 nm (solvent A, 0.1% TFA in water; B, 0.1% TFA, 20% water, 80% MeCN). Final product retention time 10.5 min; ESI-MS (m/z) = 1243.92 (100%, $[M + H]^+$).

General Procedures for the Preparation of Sulfonamide Analogues: ***5e***. Step 1: A solution of compound A or the decapeptide template, H-Dab(Boc)-Thr(tBu)-Dab(Boc)-cyclo(Dab-Dab(Boc)-DPhe-Leu-Dab(Boc)-Dab(Boc)-Thr(tBu)) (4.37g, 2.63 mmol), biphenyl-3-sulfonyl chloride (1.00 mg, 3.95 mmol), and NMM (0.44 mL, 4.0 mmol) in DMF (40 mL) was stirred at RT overnight. MS indicated the reaction was complete. The mixture was poured into water (400 mL), and a white solid formed. The solid was collected via filtration, washed with water (3 × 50 mL), and dried under high vacuum to give crude material as a white solid, 4.51 g (92% yield), which was used in the next step without purification.

Step 2: The crude product from step 1 (4.51g, 2.4 mmol) was dissolved in solution F (TFA:water:iPr_3SiH 95:2.5:2.5) (40 mL) and stirred at RT for 2 h. The reaction mixture was quenched with cold ether (400 mL), and white solid precipitate formed. The solid was isolated by removal of the supernatant after the mixture was centrifuged. The solid was dried and purified by preparative HPLC to give pure desired product as a white solid (1.394g, yield 45%). Preparative HPLC method: crude product dissolved in MeCN/water (5/95), loaded onto a 50 mm × 250 mm 10 micron Luna C18 column and purified using a 20−55% B in 60 min at a flow rate of 60 mL/min (A, 0.1% TFA in water; B, MeCN with 0.1% TFA). Product thus obtained was 80% pure and was resubjected to preparative HPLC purification again using an isocratic 40% B, and the desired product was obtained in 97% purity. Analytical method: 33% B to 43% B in 20 min at a flow rate of 1.0 mL/min on a SepaxGP-C18, 3 μm, 120 A, 4.6 mm × 150 mm column using UV 220 nm (solvent A, 0.1% TFA in water; B, 0.1% TFA, 20% water, 80% MeCN). Final product retention time 7.77 min; ESI-MS (m/z) = 633.8 (100%, $[M + 2H]^+/2$).

HRMS and NMR Data for 5a−x. *Compound* ***5a***. HRMS: $(M + 2H)^{+2}$ 595.3749, calcd 595.3744; $(M + 2Na)^{+2}$ 617.3563, calcd 617.3564. ^{1}H NMR (500 MHz, D_2O) δ 7.33 (t, J = 7.23 Hz, 2H), 7.28 (t, J = 7.27 Hz, 1H), 7.20 (d, J = 7.09 Hz, 2H), 4.79−4.73 (m, 1H), 4.51 (t, J = 8.24 Hz, 1H), 4.48−4.41 (m, 2H), 4.36 (d, J = 3.81 Hz, 1H), 4.28−4.11 (m, 7H), 3.45 (dd, J = 4.97, 13.49 Hz, 1H), 3.33−3.22 (m, 2H), 3.13−2.96 (m, 9H), 2.86−2.77 (m, 1H), 2.77−2.67 (m, 1H), 2.27 (t, J = 7.35 Hz, 2H), 2.23−1.75 (m, 10H), 1.59−1.47 (m, 2H), 1.47−1.39 (m, 1H), 1.38−1.29 (m, 1H), 1.30−1.17 (m, 5H), 1.17−1.10 (m, 6H), 1.10−0.99 (m, 2H), 0.80−0.73 (m, 7H), 0.70 (d, J = 6.37 Hz, 3H), 0.63 (d, J = 6.27 Hz, 3H).

Compound ***5b***. HRMS: $(M + 2H)^{+2}$ 602.3358, calcd 602.3353; $(M + Na)^+$ 1225.6447, calcd 1225.6452. ^{1}H NMR (500 MHz, D_2O) δ 8.41 (s, 1H), 8.09−8.03 (m, 2H), 8.01 (d, J = 8.03 Hz, 1H), 7.85 (dd, J = 1.62, 8.63 Hz, 1H), 7.74−7.61 (m, 2H), 7.37 (t, J = 7.25 Hz, 2H), 7.32 (t, J = 7.29 Hz, 1H), 7.24 (d, J = 7.15 Hz, 2H), 4.84−4.77 (m, 2H), 4.55 (t, J = 8.24 Hz, 1H), 4.51−4.43 (m, 2H), 4.38−4.30 (m, 1H), 4.30−4.22 (m, 3H), 4.22−4.15 (m, 2H), 4.13 (d, J = 4.53 Hz, 1H), 3.52 (dd, J = 4.96, 13.43 Hz, 1H), 3.39−3.26 (m, 2H), 3.26−2.98 (m, 9H), 2.93−2.82 (m, 1H), 2.81−2.72 (m, 1H), 2.45−2.34 (m, 1H), 2.34−2.06 (m, 5H), 2.06−1.78 (m, 4H), 1.52−1.43 (m, 1H), 1.42−1.34 (m, 1H), 1.22 (d, J = 6.39 Hz, 3H), 1.12 (d, J = 6.39 Hz, 3H), 0.91−0.76 (m, 1H), 0.75 (d, J = 6.28 Hz, 3H), 0.67 (d, J = 6.19 Hz, 3H).

Compound ***5c***. HRMS: $(M + 2H)^{+2}$ 615.3439, calcd 615.3431; $(M + Na)^+$ 1251.6610, calcd 1251.6609. ^{1}H NMR (500 MHz, D_2O) δ 8.08−8.04 (m, 1H), 7.95−7.89 (m, 1H), 7.83−7.78 (m, 1H), 7.76−7.70 (m, 2H), 7.63 (t, J = 7.81 Hz, 1H), 7.55 (t, J = 7.59 Hz, 2H), 7.47 (t, J = 7.39 Hz, 1H), 7.37 (t, J = 7.22 Hz, 2H), 7.32 (t, J = 7.30 Hz, 1H), 7.24 (d, J = 7.06 Hz, 2H), 4.83−4.76 (m, 2H), 4.56 (t, J = 8.25 Hz, 1H), 4.50−4.42 (m, 2H), 4.38−4.29 (m, 1H), 4.29−4.16 (m, 5H), 4.14 (d, J = 4.55 Hz, 1H), 3.52 (dd, J = 4.99, 13.43 Hz, 1H), 3.38−3.25 (m, 2H), 3.24−2.98 (m, 9H), 2.92−2.82 (m, 1H), 2.81−2.71 (m, 1H), 2.42−2.31 (m, 1H), 2.31−2.07 (m, 5H), 2.06−1.77 (m, 4H), 1.52−1.43 (m, 1H), 1.43−1.34 (m, 1H), 1.21 (d, J = 6.42 Hz, 3H), 1.14 (d, J = 6.40 Hz, 3H), 0.88−0.77 (m, 1H), 0.75 (d, J = 6.36 Hz, 3H), 0.68 (d, J = 6.26 Hz, 3H).

Compound ***5d***. HRMS: $(M + 2H)^{+2}$ 622.8486, calcd 622.8486; $(M + 2Na)^{+2}$ 644.8296, calcd 644.8305. ^{1}H NMR (500 MHz, D_2O) δ 7.66−7.60 (m, 2H), 7.57 (s, 1H), 7.47 (t, J = 7.61 Hz, 2H), 7.44−7.36 (m, 3H), 7.32 (t, J = 7.22 Hz, 2H), 7.29−7.24 (m, 2H), 7.19 (d, J = 7.10 Hz, 2H), 4.73−4.71 (m, 1H), 4.50 (t, J = 8.24 Hz, 1H), 4.44−4.36 (m, 3H), 4.32−4.25 (m, 1H), 4.24−4.11 (m, 5H), 4.10 (d, J = 4.60 Hz, 1H), 3.39 (dd, J = 4.97, 13.43 Hz, 1H), 3.30−3.16 (m, 2H), 3.16−2.94 (m, 9H), 2.85−2.75 (m, 1H), 2.74−2.64 (m, 1H), 2.28−1.99 (m, 6H), 1.99−1.71 (m, 4H), 1.47−1.37 (m, 1H), 1.38−1.28 (m, 1H), 1.17 (d, J = 6.41 Hz, 3H), 1.08 (d, J = 6.38 Hz, 3H), 0.84−0.72 (m, 1H), 0.70 (d, J = 6.38 Hz, 3H), 0.63 (d, J = 6.26 Hz, 3H).

Compound ***5e***. HRMS: $(M + 2H)^{+2}$ 633.3266, calcd 633.3266; $(M + Na)^+$ 1287.6269, calcd 1287.6279. ^{1}H NMR (500 MHz, D_2O) δ 8.12−8.09 (m, 1H), 8.03−7.98 (m, 1H), 7.88−7.83 (m, 1H), 7.77−7.68 (m, 3H), 7.56 (t, J = 7.53 Hz, 2H), 7.49 (t, J = 7.37 Hz, 1H), 7.37 (t, J = 7.24 Hz, 2H), 7.32 (t, J = 7.28 Hz, 1H), 7.24 (d, J = 7.06 Hz, 2H), 4.74−4.70 (m, 1H), 4.55 (t, J = 8.26 Hz, 1H), 4.47 (dd, J = 5.46, 8.89 Hz, 1H), 4.31−4.13 (m, 6H), 4.10 (dd, J = 4.66, 9.67 Hz, 1H), 4.03 (d, J = 3.65 Hz, 1H), 3.94−3.86 (m, 1H), 3.47 (dd, J = 4.95, 13.43 Hz, 1H), 3.33−3.19 (m, 2H), 3.18−2.96 (m, 9H), 2.91−2.80 (m, 1H), 2.79−2.69 (m, 1H), 2.30−2.05 (m, 5H), 2.04−1.75 (m, 5H), 1.53−1.43 (m, 1H), 1.43−1.34 (m, 1H), 1.16 (d, J = 6.41 Hz, 3H), 0.85 (d, J = 6.42 Hz, 3H), 0.83−0.77 (m, 1H), 0.75 (d, J = 6.32 Hz, 3H), 0.68 (d, J = 6.22 Hz, 3H).

Compound ***5f***. HRMS: $(M + 2H)^{+2}$ 615.343, calcd 615.3431. ^{1}H NMR (500 MHz, D_2O) δ 7.89−7.83 (m, 2H), 7.80−7.75 (m, 2H), 7.73−7.67 (m, 2H), 7.53−7.47 (m, 2H), 7.46−7.40 (m, 1H), 7.36−7.30 (m, 2H), 7.29−7.25 (m, 1H), 7.19 (d, J = 6.77 Hz, 2H), 4.78−4.73 (m, 2H), 4.51 (t, J = 8.22 Hz, 1H), 4.45−4.39 (m, 2H), 4.32−4.25 (m, 1H), 4.25−4.12 (m, 5H), 4.10 (d, J = 4.50 Hz, 1H), 3.47 (dd, J = 5.06, 13.48 Hz, 1H), 3.32−3.21 (m, 2H), 3.20−2.95 (m, 9H), 2.86−2.76 (m, 1H), 2.76−2.66 (m, 1H), 2.37−2.27 (m, 1H), 2.26−2.01 (m, 5H), 2.01−1.74 (m, 4H), 1.47−1.38 (m, 1H), 1.38−1.29 (m, 1H), 1.17 (d, J = 6.40 Hz, 3H), 1.09 (d, J = 6.35 Hz, 3H), 0.84−0.73 (m, 1H), 0.70 (d, J = 6.44 Hz, 3H), 0.63 (d, J = 6.30 Hz, 3H).

Compound ***5g***. HRMS: $(M + 2H)^{+2}$ 623.8382, calcd 623.8382; $(M + Na)^+$ 1268.6505, calcd 1268.6511. ^{1}H NMR (500 MHz, D_2O) δ 8.51 (d, J = 2.12 Hz, 1H), 8.22 (dd, J = 2.50, 8.76 Hz, 1H), 7.51 (t, J = 7.98 Hz, 2H), 7.42−7.28 (m, 4H), 7.25 (d, J = 7.09 Hz, 2H), 7.20 (d, J = 7.66 Hz, 2H), 7.11 (d, J = 8.77 Hz, 1H), 4.84−4.78 (m, 2H), 4.56 (t, J = 8.27 Hz, 1H), 4.48 (dd, J = 5.47, 8.93 Hz, 1H), 4.45 (d, J = 3.86 Hz, 1H), 4.36−4.11 (m, 7H), 3.51 (dd, J = 4.94, 13.43 Hz, 1H), 3.37−3.25 (m, 2H), 3.22−2.98 (m, 9H), 2.93−2.82 (m, 1H), 2.82−2.72 (m, 1H), 2.40−2.28 (m, 1H), 2.27−2.09 (m, 5H), 2.07−1.78 (m, 4H), 1.54−1.43 (m, 1H), 1.43−1.34 (m, 1H), 1.20 (d, J = 6.40 Hz, 3H), 1.17 (d, J = 6.40 Hz, 3H), 0.87−0.77 (m, 1H), 0.75 (d, J = 6.16 Hz, 3H), 0.67 (d, J = 6.15 Hz, 3H).

Compound ***5h***. HRMS: $(M + 2H)^{+2}$ 627.8409, calcd 627.8407; $(M + 2Na)^{+2}$ 649.8210, calcd 649.8227. ^{1}H NMR (500 MHz, D_2O) δ 8.29 (d, J = 1.78 Hz, 1H), 8.13 (dd, J = 1.91, 8.21 Hz, 1H), 7.74 (d, J = 8.24 Hz, 1H), 7.65 (dd, J = 1.75, 7.73 Hz, 2H), 7.62−7.55 (m, 3H), 7.36 (t, J = 7.21 Hz, 2H), 7.31 (t, J = 7.26 Hz, 1H), 7.23 (d, J = 7.07 Hz, 2H), 4.85−4.77 (m, 2H), 4.55 (t, J = 8.24 Hz, 1H), 4.51−4.44 (m, 2H), 4.38−4.12 (m, 7H), 3.52 (dd, J = 5.00, 13.43 Hz, 1H), 3.38−3.26 (m, 2H), 3.25−2.99 (m, 9H), 2.94−2.83 (m, 1H), 2.83−2.72 (m, 1H), 2.42−2.31 (m, 1H), 2.31−2.08 (m, 5H), 2.08−1.79 (m, 4H), 1.52−1.42 (m, 1H), 1.42−1.33 (m, 1H), 1.22 (d, J = 6.38 Hz, 3H), 1.15 (d, J = 6.41 Hz, 3H), 0.90−0.76 (m, 1H), 0.74 (d, J = 6.24 Hz, 3H), 0.67 (d, J = 6.18 Hz, 3H).

Compound ***5i***. HRMS: $(M + 2H)^{+2}$ 627.8407, calcd 627.8407; $(M + 2Na)^{+2}$ 649.8219, calcd 649.8227. ^{1}H NMR (500 MHz, D_2O) δ 8.00 (d, J = 8.12 Hz, 1H), 7.96 (d, J = 1.28 Hz, 1H), 7.90 (dd, J = 1.67, 8.11 Hz, 1H), 7.65 (dd, J = 1.58, 7.87 Hz, 2H), 7.61−7.53 (m, 3H), 7.37 (t, J = 7.23 Hz, 2H), 7.32 (t, J = 7.26 Hz, 1H), 7.24 (d, J = 7.08 Hz, 2H), 4.87−4.76 (m, 2H), 4.56 (t, J = 8.25 Hz, 1H), 4.51−4.44 (m, 2H), 4.36−4.17 (m, 6H), 4.15 (d, J = 4.54 Hz, 1H), 3.51 (dd, J = 4.97, 13.43 Hz, 1H), 3.37−3.24 (m, 2H), 3.18 (t, J = 7.75 Hz, 2H), 3.14−2.99 (m, 7H), 2.91−2.83 (m, 1H), 2.82−2.72 (m, 1H), 2.41−2.29 (m,

1H), 2.29−2.08 (m, 5H), 2.07−1.77 (m, 4H), 1.53−1.44 (m, 1H), 1.43−1.33 (m, 1H), 1.20 (d, J = 6.40 Hz, 3H), 1.15 (d, J = 6.40 Hz, 3H), 0.88−0.77 (m, 1H), 0.75 (d, J = 6.25 Hz, 3H), 0.67 (d, J = 6.19 Hz, 3H).

Compound ***5j***. HRMS: $(M + 2H)^{+2}$ 630.3493, calcd 630.3484; $(M + Na)^{+}$ 1281.6722, calcd 1281.6715. ^{1}H NMR (500 MHz, D_2O) δ 7.87 (dd, J = 2.40, 8.69 Hz, 1H), 7.78 (d, J = 2.39 Hz, 1H), 7.57−7.47 (m, 4H), 7.47−7.41 (m, 1H), 7.37 (t, J = 7.23 Hz, 2H), 7.32 (t, J = 7.30 Hz, 1H), 7.24 (d, J = 8.64 Hz, 3H), 4.84−4.77 (m, 2H), 4.56 (t, J = 8.25 Hz, 1H), 4.51−4.41 (m, 2H), 4.37−4.29 (m, 1H), 4.29−4.23 (m, 3H), 4.23−4.16 (m, 2H), 4.15 (d, J = 4.58 Hz, 1H), 3.87 (s, 3H), 3.51 (dd, J = 4.99, 13.44 Hz, 1H), 3.40−3.26 (m, 2H), 3.23−2.98 (m, 9H), 2.93−2.82 (m, 1H), 2.82−2.71 (m, 1H), 2.39−2.29 (m, 1H), 2.29−2.07 (m, 5H), 2.07−1.79 (m, 4H), 1.53−1.43 (m, 1H), 1.43−1.34 (m, 1H), 1.20 (d, J = 6.41 Hz, 3H), 1.14 (d, J = 6.40 Hz, 3H), 0.89−0.77 (m, 1H), 0.75 (d, J = 6.32 Hz, 3H), 0.68 (d, J = 6.22 Hz, 3H).

Compound ***5k***. HRMS: $(M + 2H)^{+2}$ 630.3494, calcd 630.3484; $(M + 2Na)^{+2}$ 652.3317, calcd 652.3303. ^{1}H NMR (500 MHz, D_2O) δ 7.71 (d, J = 7.21 Hz, 2H), 7.68−7.65 (m, 1H), 7.53 (t, J = 7.51 Hz, 2H), 7.50−7.44 (m, 2H), 7.40−7.34 (m, 3H), 7.32 (t, J = 7.28 Hz, 1H), 7.24 (d, J = 7.08 Hz, 2H), 4.83−4.76 (m, 2H), 4.55 (t, J = 8.25 Hz, 1H), 4.49−4.43 (m, 2H), 4.38−4.30 (m, 1H), 4.30−4.22 (m, 3H), 4.22−4.15 (m, 2H), 4.13 (d, J = 4.51 Hz, 1H), 3.93 (s, 3H), 3.52 (dd, J = 5.02, 13.43 Hz, 1H), 3.37−3.26 (m, 2H), 3.23−2.98 (m, 9H), 2.92−2.83 (m, 1H), 2.83−2.73 (m, 1H), 2.42−2.31 (m, 1H), 2.31−2.08 (m, 5H), 2.07−1.78 (m, 4H), 1.51−1.42 (m, 1H), 1.42−1.33 (m, 1H), 1.22 (d, J = 6.41 Hz, 3H), 1.13 (d, J = 6.41 Hz, 3H), 0.85−0.76 (m, 1H), 0.74 (d, J = 6.02 Hz, 3H), 0.67 (d, J = 6.05 Hz, 3H).

Compound ***5l***. HRMS: $(M + 2H)^{+2}$ 630.3481, calcd 630.3484; $(M + 2Na)^{+2}$ 652.3315, calcd 652.3303. ^{1}H NMR (500 MHz, D_2O) δ 8.02 (d, J = 2.39 Hz, 1H), 7.87 (dd, J = 2.42, 8.71 Hz, 1H), 7.68 (d, J = 7.43 Hz, 2H), 7.52 (t, J = 7.71 Hz, 2H), 7.45−7.27 (m, 5H), 7.24 (d, J = 7.15 Hz, 2H), 4.81−4.75 (m, 2H), 4.56 (t, J = 8.24 Hz, 1H), 4.51−4.44 (m, 2H), 4.38−4.11 (m, 7H), 3.99 (s, 3H), 3.53 (dd, J = 5.07, 13.46 Hz, 1H), 3.38−3.24 (m, 2H), 3.23−2.96 (m, 9H), 2.90−2.81 (m, 1H), 2.81−2.71 (m, 1H), 2.42−2.31 (m, 1H), 2.29−2.05 (m, 5H), 2.05−1.79 (m, 4H), 1.53−1.44 (m, 1H), 1.43−1.34 (m, 1H), 1.23 (d, J = 6.39 Hz, 3H), 1.13 (d, J = 6.40 Hz, 3H), 0.87−0.77 (m, 1H), 0.75 (d, J = 6.21 Hz, 3H), 0.68 (d, J = 6.13 Hz, 3H).

Compound ***5m***. HRMS: $(M + 2H)^{+2}$ 632.3241, calcd 632.3236; $(M + 2Na)^{+2}$ 654.3070, calcd 654.3056. ^{1}H NMR (500 MHz, D_2O) δ 7.80 (d, J = 2.17 Hz, 1H), 7.77 (dd, J = 2.26, 8.37 Hz, 1H), 7.68 (d, J = 8.36 Hz, 1H), 7.56−7.46 (m, 5H), 7.37 (t, J = 7.23 Hz, 2H), 7.32 (t, J = 7.28 Hz, 1H), 7.24 (d, J = 7.09 Hz, 2H), 4.83−4.76 (m, 2H), 4.56 (t, J = 8.26 Hz, 1H), 4.51−4.43 (m, 2H), 4.36−4.17 (m, 6H), 4.15 (d, J = 4.56 Hz, 1H), 3.51 (dd, J = 4.98, 13.44 Hz, 1H), 3.38−3.25 (m, 2H), 3.22−2.99 (m, 9H), 2.92−2.82 (m, 1H), 2.82−2.71 (m, 1H), 2.39−2.28 (m, 1H), 2.28−2.07 (m, 5H), 2.07−1.77 (m, 4H), 1.53−1.43 (m, 1H), 1.43−1.33 (m, 1H), 1.19 (d, J = 6.41 Hz, 3H), 1.15 (d, J = 6.40 Hz, 3H), 0.89−0.77 (m, 1H), 0.75 (d, J = 6.32 Hz, 3H), 0.68 (d, J = 6.22 Hz, 3H).

Compound ***5n***. HRMS: $(M + 2H)^{+2}$ 632.8213, calcd 632.8213; $(M + 2Na)^{+2}$ 655.3051, calcd 655.3046. ^{1}H NMR (500 MHz, D_2O) δ 8.83 (d, J = 5.44 Hz, 1H), 8.58 (t, J = 7.89 Hz, 1H), 8.11 (d, J = 7.91 Hz, 1H), 8.07−7.96 (m, 3H), 7.81 (d, J = 8.30 Hz, 1H), 7.38 (t, J = 7.26 Hz, 2H), 7.32 (t, J = 7.28 Hz, 1H), 7.25 (d, J = 7.10 Hz, 2H), 4.86−4.79 (m, 2H), 4.56 (t, J = 8.28 Hz, 1H), 4.52−4.42 (m, 2H), 4.35−4.12 (m, 7H), 3.50 (dd, J = 4.95, 13.46 Hz, 1H), 3.39−3.26 (m, 2H), 3.24−2.99 (m, 9H), 2.94−2.82 (m, 1H), 2.82−2.72 (m, 1H), 2.39−2.28 (m, 1H), 2.28−2.08 (m, 5H), 2.07−1.77 (m, 4H), 1.53−1.43 (m, 1H), 1.43−1.33 (m, 1H), 1.20 (d, J = 6.34 Hz, 3H), 1.17 (d, J = 6.40 Hz, 3H), 0.85−0.77 (m, 1H), 0.74 (d, J = 6.04 Hz, 3H), 0.67 (d, J = 6.08 Hz, 3H).

Compound ***5o***. HRMS: $(M + 2H)^{+2}$ 644.8216, calcd 644.8213. ^{1}H NMR (500 MHz, D_2O) δ 7.87 (d, J = 8.40 Hz, 2H), 7.84−7.79 (m, 2H), 7.70 (d, J = 8.94 Hz, 1H), 7.67 (d, J = 8.40 Hz, 2H), 7.37 (t, J = 7.25 Hz, 2H), 7.32 (t, J = 7.27 Hz, 1H), 7.24 (d, J = 7.09 Hz, 2H), 4.83−4.76 (m, 2H), 4.56 (t, J = 8.24 Hz, 1H), 4.50−4.41 (m, 2H), 4.36−4.17 (m, 6H), 4.15 (d, J = 4.55 Hz, 1H), 3.51 (dd, J = 4.96, 13.44 Hz, 1H), 3.36−3.24 (m, 2H), 3.23−2.99 (m, 9H), 2.92−2.82 (m, 1H), 2.82−2.72 (m, 1H), 2.39−2.28 (m, 1H), 2.28−2.08 (m, 5H), 2.06−1.76 (m, 4H), 1.51−1.42 (m, 1H), 1.43−1.33 (m, 1H), 1.21−1.17 (m, 3H), 1.15 (d, J = 6.41 Hz, 3H), 0.91−0.77 (m, 1H), 0.75 (d, J = 6.33 Hz, 3H), 0.67 (d, J = 6.24 Hz, 3H).

Compound ***5p***. HRMS: $(M + 2H)^{+2}$ 615.8399, calcd 615.8407. ^{1}H NMR (500 MHz, D_2O) δ 8.71 (d, J = 5.20 Hz, 1H), 8.10 (d, J = 0.63 Hz, 1H), 7.89 (d, J = 7.72 Hz, 2H), 7.69 (d, J = 5.20 Hz, 1H), 7.50−7.60 (m, 3H), 7.34 (t, J = 7.30 Hz, 2H), 7.29 (t, J = 6.90 Hz, 1H), 7.21 (d, J = 7.57 Hz, 2H), 4.77−4.81 (m, 2H), 4.42−4.49 (m, 3H), 4.30−4.37 (m, 1H), 4.18−4.30 (m, 4H), 4.13 (dd, J = 3.39, 11.43 Hz, 1H), 4.09 (d, J = 4.57 Hz, 1H), 3.52 (dd, J = 4.97, 13.32 Hz, 1H), 3.28−3.39 (m, 2H), 2.99−3.21 (m, 8H), 2.89−2.99 (m, 2H), 2.81−2.89 (m, 1H), 2.32−2.43 (m, 1H), 2.10−2.32 (m, 5H), 1.89−2.10 (m, 3H), 1.76−1.89 (m, 1H), 1.36−1.48 (m, 1H), 1.24−1.36 (m, 1H), 1.20 (d, J = 6.31 Hz, 3H), 1.13 (d, J = 6.46 Hz, 3H), 0.67 (d, J = 6.15 Hz, 3H), 0.59 (d, J = 5.67 Hz, 3H), 0.50−0.57 (m, 1H).

Compound ***5q***. HRMS: $(M + 2H)^{+2}$ 615.8405, calcd 615.8407; $(M + Na)^{+}$ 1252.6556, calcd 1252.6561. ^{1}H NMR (500 MHz, D_2O) δ 9.12 (d, J = 2.00 Hz, 1H), 9.04 (d, J = 1.84 Hz, 1H), 8.89−8.81 (m, 1H), 7.78 (d, J = 6.82 Hz, 2H), 7.66−7.52 (m, 3H), 7.37 (t, J = 7.24 Hz, 2H), 7.32 (t, J = 7.29 Hz, 1H), 7.24 (d, J = 7.09 Hz, 2H), 4.85−4.77 (m, 2H), 4.55 (t, J = 8.26 Hz, 1H), 4.52−4.45 (m, 2H), 4.37−4.13 (m, 7H), 3.51 (dd, J = 4.98, 13.45 Hz, 1H), 3.38−3.26 (m, 2H), 3.26−2.98 (m, 9H), 2.92−2.82 (m, 1H), 2.82−2.72 (m, 1H), 2.42−2.08 (m, 6H), 2.07−1.79 (m, 4H), 1.53−1.43 (m, 1H), 1.43−1.34 (m, 1H), 1.22 (d, J = 6.40 Hz, 3H), 1.16 (d, J = 6.41 Hz, 3H), 0.85−0.77 (m, 1H), 0.75 (d, J = 6.17 Hz, 3H), 0.67 (d, J = 6.13 Hz, 3H).

Compound ***5r***. HRMS: $(M + 2H)^{+2}$ 630.8468, calcd 630.8460; $(M + Na)^{+}$ 1282.6658, calcd 1282.6667. ^{1}H NMR (500 MHz, D_2O) δ 8.81 (d, J = 6.16 Hz, 1H), 8.54 (d, J = 1.00 Hz, 1H), 8.14 (dd, J = 1.68, 6.19 Hz, 1H), 7.92 (d, J = 8.96 Hz, 2H), 7.37 (t, J = 7.23 Hz, 2H), 7.32 (t, J = 7.28 Hz, 1H), 7.27−7.20 (m, 4H), 4.88−4.78 (m, 2H), 4.55 (t, J = 8.25 Hz, 1H), 4.52−4.46 (m, 2H), 4.37−4.14 (m, 7H), 3.93 (s, 3H), 3.51 (dd, J = 4.95, 13.44 Hz, 1H), 3.38−3.26 (m, 2H), 3.25−2.98 (m, 9H), 2.93−2.83 (m, 1H), 2.82−2.73 (m, 1H), 2.42−2.09 (m, 6H), 2.08−1.80 (m, 4H), 1.53−1.42 (m, 1H), 1.42−1.33 (m, 1H), 1.22 (d, J = 6.32 Hz, 3H), 1.16 (d, J = 6.41 Hz, 3H), 0.85−0.75 (m, 1H), 0.74 (d, J = 5.75 Hz, 3H), 0.67 (d, J = 5.94 Hz, 3H).

Compound ***5s***. HRMS: $(M + 2H)^{+2}$ 630.8465, calcd 630.8460; $(M + Na)^{+}$ 1282.6654, calcd 1282.6667. ^{1}H NMR (500 MHz, D_2O) δ 8.01 (dd, J = 1.51, 7.94 Hz, 2H), 7.75 (d, J = 0.97 Hz, 1H), 7.59−7.50 (m, 3H), 7.37 (t, J = 7.24 Hz, 2H), 7.32 (t, J = 7.26 Hz, 1H), 7.24 (d, J = 7.10 Hz, 2H), 7.14 (d, J = 0.97 Hz, 1H), 4.83−4.77 (m, 2H), 4.55 (t, J = 8.24 Hz, 1H), 4.50−4.43 (m, 2H), 4.37−4.29 (m, 1H), 4.29−4.16 (m, 5H), 4.14 (d, J = 4.53 Hz, 1H), 4.05 (s, 3H), 3.52 (dd, J = 5.01, 13.44 Hz, 1H), 3.38−3.25 (m, 2H), 3.23−2.99 (m, 9H), 2.91−2.82 (m, 1H), 2.81−2.72 (m, 1H), 2.41−2.30 (m, 1H), 2.30−2.06 (m, 5H), 2.05−1.78 (m, 4H), 1.52−1.42 (m, 1H), 1.42−1.33 (m, 1H), 1.22 (d, J = 6.40 Hz, 3H), 1.14 (d, J = 6.41 Hz, 3H), 0.86−0.77 (m, 1H), 0.74 (d, J = 6.31 Hz, 3H), 0.67 (d, J = 6.21 Hz, 3H).

Compound ***5t***. HRMS: $(M + 2H)^{+2}$ 616.3385, calcd 616.3384; $(M + 2Na)^{+2}$ 638.3199, calcd 638.3203. ^{1}H NMR (500 MHz, D_2O) δ 9.40 (d, J = 1.98 Hz, 1H), 8.44 (d, J = 1.99 Hz, 1H), 8.04−7.90 (m, 2H), 7.65−7.53 (m, 3H), 7.32 (t, J = 7.24 Hz, 2H), 7.27 (t, J = 7.27 Hz, 1H), 7.19 (d, J = 7.09 Hz, 2H), 4.79−4.72 (m, 2H), 4.51 (t, J = 8.25 Hz, 1H), 4.45−4.39 (m, 2H), 4.31−4.06 (m, 7H), 3.47 (dd, J = 4.99, 13.44 Hz, 1H), 3.32−3.21 (m, 2H), 3.20−2.93 (m, 9H), 2.87−2.77 (m, 1H), 2.77−2.67 (m, 1H), 2.39−2.27 (m, 1H), 2.27−2.02 (m, 5H), 2.02−1.74 (m, 4H), 1.48−1.38 (m, 1H), 1.38−1.29 (m, 1H), 1.17 (d, J = 6.40 Hz, 3H), 1.10 (d, J = 6.40 Hz, 3H), 0.83−0.72 (m, 1H), 0.70 (d, J = 6.37 Hz, 3H), 0.62 (d, J = 6.25 Hz, 3H).

Compound ***5u***. HRMS: $(M + 2H)^{+2}$ 632.8214, calcd 632.8213; $(M + 2Na)^{+2}$ 654.8023, calcd 654.8032. ^{1}H NMR (500 MHz, D_2O) δ 8.86 (dd, J = 0.58, 5.55 Hz, 1H), 8.19−8.11 (m, 1H), 7.99 (dd, J = 1.67, 5.55 Hz, 1H), 7.69−7.61 (m, 1H), 7.60−7.48 (m, 3H), 7.37 (t, J = 7.23 Hz, 2H), 7.32 (t, J = 7.29 Hz, 1H), 7.24 (d, J = 7.07 Hz, 2H), 4.85−4.76 (m, 2H), 4.55 (t, J = 8.26 Hz, 1H), 4.52−4.44 (m, 2H), 4.36−4.12 (m, 7H), 3.51 (dd, J = 4.98, 13.43 Hz, 1H), 3.38−3.26 (m, 2H), 3.24−2.99 (m, 9H), 2.92−2.83 (m, 1H), 2.82−2.73 (m, 1H), 2.41−2.30 (m, 1H), 2.30−2.09 (m, 5H), 2.09−1.79 (m, 4H), 1.52−

dx.doi.org/10.1021/jm400416u | J. Med. Chem. 2013, 56, 5079−5093

1.43 (m, 1H), 1.43−1.34 (m, 1H), 1.21 (d, J = 6.40 Hz, 3H), 1.16 (d, J = 6.40 Hz, 3H), 0.86−0.76 (m, 1H), 0.74 (d, J = 6.12 Hz, 3H), 0.67 (d, J = 6.11 Hz, 3H).

Compound ***5v***. HRMS: $(M + 2H)^{+2}$ 632.8220, calcd 632.8213; $(M + 2Na)^{+2}$ 654.8033, calcd 654.8032. ^{1}H NMR (500 MHz, D_2O) δ 8.82 (d, J = 5.60 Hz, 1H), 8.31 (d, J = 0.73 Hz, 1H), 7.96 (dd, J = 1.55, 5.57 Hz, 1H), 7.93 (t, J = 1.69 Hz, 1H), 7.86−7.79 (m, 1H), 7.65−7.59 (m, 1H), 7.57 (t, J = 7.86 Hz, 1H), 7.37 (t, J = 7.23 Hz, 2H), 7.32 (t, J = 7.29 Hz, 1H), 7.24 (d, J = 7.07 Hz, 2H), 4.85−4.78 (m, 2H), 4.55 (t, J = 8.27 Hz, 1H), 4.51−4.45 (m, 2H), 4.38−4.12 (m, 7H), 3.52 (dd, J = 4.97, 13.44 Hz, 1H), 3.39−3.27 (m, 2H), 3.25−2.99 (m, 9H), 2.94−2.83 (m, 1H), 2.83−2.73 (m, 1H), 2.43−2.32 (m, 1H), 2.31−2.08 (m, 5H), 2.08−1.79 (m, 4H), 1.52−1.42 (m, 1H), 1.42−1.33 (m, 1H), 1.23 (d, J = 6.40 Hz, 3H), 1.15 (d, J = 6.41 Hz, 3H), 0.84−0.76 (m, 1H), 0.74 (d, J = 5.92 Hz, 3H), 0.67 (d, J = 6.03 Hz, 3H).

Compound ***5w***. HRMS: $(M + 2H)^{+2}$ 632.8212, calcd 632.8213. ^{1}H NMR (500 MHz, D_2O) δ 8.80 (d, J = 5.52 Hz, 1H), 8.28 (s, 1H), 7.93−7.84 (m, 3H), 7.62 (d, J = 8.55 Hz, 2H), 7.42−7.28 (m, 3H), 7.24 (d, J = 7.15 Hz, 2H), 4.86−4.77 (m, 2H), 4.55 (t, J = 8.23 Hz, 1H), 4.51−4.44 (m, 2H), 4.37−4.11 (m, 7H), 3.51 (dd, J = 4.97, 13.43 Hz, 1H), 3.38−3.26 (m, 2H), 3.25−2.99 (m, 9H), 2.93−2.81 (m, 1H), 2.81−2.71 (m, 1H), 2.42−2.31 (m, 1H), 2.31−2.07 (m, 5H), 2.06−1.78 (m, 4H), 1.53−1.43 (m, 1H), 1.42−1.34 (m, 1H), 1.22 (d, J = 6.40 Hz, 3H), 1.15 (d, J = 6.39 Hz, 3H), 0.88−0.77 (m, 1H), 0.75 (d, J = 6.29 Hz, 3H), 0.67 (d, J = 6.20 Hz, 3H).

Compound ***5x***. HRMS: $(M + 3H)^{+3}$ 416.2291, calcd 416.2279; $(M + 2H)^{+2}$ 623.8390, calcd 623.8382; $(M + Na)^{+}$ 1268.65 calcd 1268.6511. ^{1}H NMR (600 MHz, D_2O) δ 8.40 (dd, J = 2.6, 0.6 Hz, 1H), 8.14 (dd, J = 9.6, 2.6 Hz, 1H), 7.71−7.64 (m, 3H), 7.53−7.49 (m, 2H), 7.47−7.44 (m, 2H), 7.43−7.39 (m, 1H), 7.33 (d, J = 6.9 Hz, 2H), 6.85 (dd, J = 9.6, 0.6 Hz, 1H), 4.88 (dd, J = 8.7, 5.0 Hz, 1H), 4.76 (dd, J = 9.3, 5.3 Hz, 1H), 4.64 (t, J = 8.2 Hz, 1H), 4.56 (dd, J = 8.9, 5.5 Hz, 1H), 4.52 (d, J = 3.9 Hz, 1H), 4.41−4.23 (m, 7H), 3.58 (dd, J = 13.5, 5.0 Hz, 1H), 3.42−3.35 (m, 2H), 3.27−3.09 (m, 9H), 2.99−2.91 (m, 1H), 2.89−2.81 (m, 1H), 2.42−2.18 (m, 6H), 2.13−1.88 (m, 4H), 1.59−1.52 (m, 1H), 1.51−1.43 (m, 1H), 1.27 (d, J = 6.4 Hz, 3H), 1.25 (d, J = 6.4 Hz, 3H), 0.96−0.86 (m, 1H), 0.83 (d, J = 6.5 Hz, 3H), 0.76 (d, J = 6.4 Hz, 3H).

Synthesis of Noncommercial Biaryl Acid Intermediates. *2-Methoxy-6-phenyl-isonicotinic Acid.* Step 1: Citrazinic acid (2.00 g, 12.9 mmol, 1.0 equiv) and phosphorus oxybromide (11.19 g, 3.0 equiv) were heated at 180 °C under nitrogen for 2 h. The reaction mixture was cooled to RT and ice water added cautiously, and the resulting mixture was left at RT for 12 h before extracting with EtOAc (4 × 100 mL). The combined organic layer was dried over sodium sulfate, filtered, and concentrated to dryness to afford 3.0 g (83% yield) of 2,6-dibromo-isonicotinic acid as a light-brown solid.

Step 2: 2,6-Dibromo-isonicotinic acid (3.00 g, 1 equiv) and sodium methoxide (2.88 g, 5 equiv) were dissolved in anhydrous MeOH (21 mL) and heated to reflux for 48 h. The mixture was cooled to RT, dissolved in 20 mL water, and adjusted to pH ∼ 3 with 3 N HCl. This was then extracted with EtOAc (3 × 50 mL). The combined organic layer was dried over sodium sulfate, filtered, and concentrated to dryness to afford 2.3 g (93% yield) of 2-bromo-6-methoxy-isonicotinic acid as a light-brown solid.

Step 3: To a mixture of phenylboronic acid (394 mg, 1.5 equiv) and crude acid of step 2 (500 mg, 1.0 equiv) in dioxane (5 mL) was added 2 M Na_2CO_3 (3.76 mL, 3.5 equiv) and $Pd(PPh_3)_4$ (248 mg, 0.1 equiv) in a 35 mL Q-tube (Sigma-Aldrich). The mixture was stirred at 180 °C for 20 min. The crude product was then filtered through Celite. The Celite was subsequently rinsed several times with water (2 × 5 mL), and the filtrate was poured into a separatory funnel and extracted with heptane (3 × 20 mL) and then with EtOAc (1 × 20 mL) to remove some of the unwanted organic materials. The aqueous layer was acidified to pH ∼ 2 with 1 N HCl and extracted with EtOAc (3 × 20 mL). The combined EtOAc layers were dried over anhydrous sodium sulfate, filtered, and concentrated to dryness to afford 412 mg of crude yellow solid. The crude product was purified by flash chromatography using an Analogix SF25 40 g column with a gradient of 0−5% of MeOH/DCM. Relevant fractions were combined and concentrated to dryness to afford 200 mg (41% yield) of desired product as a white solid. ^{1}H NMR (400 MHz, DMSO-d_6) δ 13.69 (br s, 1H), 8.06−8.21 (m, 2H), 7.90 (d, J = 1.17 Hz, 1 H), 7.38−7.62 (m, 3H), 7.16 (d, J = 0.98 Hz, 1H), 4.01 (s, 3H).

4-Chloro-3-pyridin-2-yl-benzoic Acid. Step 1: 5-Ethoxycarbonyl-2-chlorophenyl boronic acid (2.05 g, 8.87 mmol, 1.0 equiv) was dissolved in a solution of degassed 1,4-dioxane/water (5:1, 49.0 mL), followed by 2-chloropyridine (0.917 mL, 9.69 mmol, 1.1 equiv), potassium carbonate (3.65g, 26.4 mmol, 3.0 equiv), and $Pd(PPh_3)_4$ (1.04g, 0.881 mmol, 0.10 equiv), the reaction was stirred at 83 °C for 3.0 h. The mixture was cooled to RT. Water (30.0 mL) and ethyl acetate (150.0 mL) were added. The organics were separated and the aqueous layer extracted with ethyl acetate (3 × 80 mL). The combined organics were dried over sodium sulfate, filtered, and concentrated. The crude product was purified by column chromatography (Analogix SF-65 400 g column) using 8−50% EtOAc/heptane gradient to yield the desired product (1.01g, 3.86 mmol, 43.9% yield).

Step 2: The ethyl ester from step 1 (1.01g, 3.86 mmol, 1.0 equiv) was dissolved in a solution of water:THF (1:2, 60 mL) and treated with LiOH hydrate (0.277 g, 11.6 mmol, 3.0 equiv). The solution was stirred at RT for 4 h, then extracted with heptanes (2 × 20 mL). The mixture was then saturated with sodium chloride, and pH was adjusted stepwise from 5 to 1 with 1 N HCl. This mixture was subsequently extracted with EtOAc (9 × 50 mL). The combined EtOAc layer was dried over sodium sulfate, filtered, and concentrated to yield the desired product (0.650 g, 62.5% yield). ^{1}H NMR (400 MHz, DMSO-d_6) δ 13.26 (br s, 1H), 8.55−8.85 (m, 1H), 7.87−8.17 (m, 3H), 7.63−7.78 (m, 2H), 7.44 (ddd, J = 7.61, 4.88, 1.17 Hz, 1H).

5-Methoxy-biphenyl-3-carboxylic Acid. Step 1: A mixture of 1,3-dibromo-5-methoxy-benzene (5g, 18.8 mmol), $Pd(dppf)Cl_2$ (4g, 5.47 mmol), and TEA (3.8g, 37.55 mmol) in MeOH/DMF (75 mL/75 mL) was stirred at 50 °C under 50 psi CO for 16 h. TLC (petroleum ether/EtOAc 10/1) indicated little starting material remained. The mixture was cooled to RT and filtered. The filtrate was concentrated, and the residue was dissolved in water (100 mL) and extracted with EtOAc (3 × 100 mL). The combined organic layer was washed with brine, dried over sodium sulfate, filtrated, and concentrated. The residue was purified via flash column chromatography to give an oil product 3-bromo-5-methoxy-benzoic acid methyl ester (1.2 g, 24.5% yield).

Step 2: A mixture of 3-bromo-5-methoxy-benzoic acid methyl ester (830 mg, 3.39 mmol), phenylboronic acid (573 mg, 4.07 mmol), $Pd(PPh_3)_4$ (200 mg, 0.173 mmol), and sodium carbonate (900 mg, 8.49 mmol) in DME/water (20/20 mL) was heated to reflux with stirring for 16 h under nitrogen. TLC (petroleum ether/EtOAc 20/1) showed the reaction was complete. The reaction mixture was filtered, and the filtrate was extracted with EtOAc (4 × 50 mL). The combined organic layer was washed with brine, dried over sodium sulfate, and concentrated to give 5-methoxy-biphenyl-3-carboxylic acid methyl ester (1.3 g), which was purified via flash chromatography to give the product as an oil (600 mg, 73.2% yield).

Step 3: To a mixture of 5-methoxy-biphenyl-3-carboxylic acid methyl ester (600 mg, 2.49 mmol) in THF/water (30 mL/30 mL) was added LiOH hydrate (312 mg, 7.43 mmol) at 0−5 °C. After the addition, the mixture was stirred at RT for 16 h. TLC (petroleum ether/EtOAc 10/1) showed the reaction was complete. The mixture was concentrated, and the residue was dissolved in water (150 mL) and extracted with ether (3 × 150 mL). The aqueous layer was acidified pH to 2−3 with 1 M HCl and extracted with EtOAc (6 × 50 mL), and the combined organic layers were dried, filtered, and concentrated to give the desired compound (540 mg, 95.6% yield) as a white solid. ^{1}H NMR (400 MHz, DMSO-d_6) δ 13.14 (br s, 1H), 7.70−7.77 (m, 3H), 7.39−7.49 (m, 5H), 3.88 (s, 3H).

6-Oxo-1-phenyl-1,6-dihydropyridine-3-carboxylic Acid. A stirred solution of methyl 2-oxo-2*H*-pyran-5-carboxylate (500 mg, 3.246 mmol) and aniline (604.2 mg, 6.492 mmol) in pyridine (5 mL) was heated to 80 °C and stirred overnight. TLC (petroleum ether/EtOAc = 2:1) showed the starting material was consumed completely. The reaction solution was cooled to room temperature, evaporated to dryness, and purified via chromatography (petroleum ether/EtOAc

gradient) to give methyl 6-oxo-1-phenyl-1,6-dihydropyridine-3-carboxylate (290 mg, 39% yield) as a yellow solid. This material was subsequently dissolved in MeOH (3 mL) and to this was added aqueous LiOH (159.6 mg, 3.799 mmol, dissolved in 1 mL water). After the addition, the resulting solution was stirred at RT overnight. LC-MS showed the starting material was consumed completely. The bulk of the solvent was removed in vacuo, and the resulting residue was diluted with water (20 mL) and then extracted with MTBE (20 mL). The aqueous layer was adjusted to pH = 2−3 with 1 M HCl solution and extracted with EtOAc (3 × 20 mL). The combined EtOAc extracts were evaporated to dryness to give the title compound (156 mg, 57.3% yield) as a yellow solid. ^{1}H NMR: (400 MHz, methanol-d_4): δ 8.317−8.311 (d, 1H), 8.068−8.038 (m, 1H), 7.593−7.521 (m, 3H), 7.450−7.429 (m, 2H), 6.648−6.624 (d, 1H).

MIC and MBC Determinations. The in vitro antibacterial activity of test compounds was evaluated by MBC and MIC testing according to Clinical and Laboratory Standards Institute (CLSI). The following bacterial strains were used in these MIC determinations: PA-1646 and AB-1649 are polymyxin-resistant clinical isolates of *P. aeruginosa* and *A. baumannii*, respectively, obtained from JMI laboratories (www.jmilabs.com); PA01 is a *P. aeruginosa* lab strain (www.fems-microbiology.org); AB-3167 is clinical isolate of *A. baumannii* obtained from IHMA (www.ihmainc.com); KP-3700 is an ESBL+ clinical isolate of *K. pneumoniae* obtained in 2006; EC-1 is a mouse virulent strain of *E. coli*.

hRPTEC Cytotoxicity Assay. Human renal proximal tubule epithelial cells (hRPTEC) were obtained from Lonza (Walkersville, MD) and cultured in REGM (Renal Epithelial Cell Basal Medium supplemented with human epithelial growth factor, hydrocortisone, epinephrine, insulin, triiodothyronine, transferrin, gentamycin/amphotericin-B, and fetal bovine serum). The hRPTEC cells were seeded into 96-well plates and incubated at 37 °C in 5% CO_2. Following a growth period of 72 h, cells were treated with compounds at 100, 67, 44, 30, 20, and 13 μM aqueous solution for 24 h at 37 °C in 5% CO_2. The cell supernatant was then harvested for determination of LDH (lactate dehydrogenase) production. The Cytotoxicity Detection Kit from Roche was used for the measurement of LDH activity released from damaged cells. The toxic concentration 50% (TC_{50}, μM) values were determined for each compound and compared to the control compounds (PMB was used as a positive control and PMBN was used as negative control).

Toxicology Studies in Rats and Dogs. All studies were conducted in accordance with the current guidelines for animal welfare (ILAR Guide for the Care and Use of Laboratory Animals, 1996; Animal Welfare Act, 1966, as amended in 1970, 1976, and 1985, 9 CFR Parts 1, 2, and 3). The procedures used in these studies were reviewed and approved by the Institutional Animal Care and Use Committee of the testing facility.

Rat Studies. Rat studies were conducted utilizing male Wistar Han IGS rats (CRL:WI [HAN]) with an age range of 6−9 weeks at study initiation. Rats were administered intravenous bolus doses twice daily to achieve total daily doses of 0 (0.9% sterile saline), 0.4, 4, or 10 mg/kg/day polymyxin B (PMB) or 0 (0.9% sterile saline), 4 or 8 mg/kg/day **5x** with at least 6 h between each dose for 7 days. Plasma samples were collected on days 1 and 7 for toxicokinetic analysis. Animals were euthanized and necropsied the day after the last dose. After gross examination, the kidneys were weighed, collected, processed, and examined microscopically. Microscopic lesions were graded on a scale of 1−5 as minimal, mild, moderate, marked, or severe.

Dog Studies. Dog studies were conducted utilizing male and female Beagle dogs with a body weight range of 5−11 kg at study initiation. Dogs were administered intravenous bolus doses twice daily to achieve total daily doses of 0 (0.9% sterile saline), 1, or 6 mg/kg/day PMB or 0 (0.9% sterile saline), 5, 11, or 20 mg/kg/day **5x** with at least 6 h between each dose for 7 days. Plasma samples were collected on days 1 and 7 for toxicokinetic analysis. Animals were euthanized and necropsied the day after the last dose. After gross examination, the kidneys were weighed, collected, processed, and examined microscopically. Microscopic lesions were graded on a scale of 1−5 as minimal, mild, moderate, marked, or severe.

In Vivo PK/PD Studies. The comparative in vivo pharmacodynamics of **5x** and PMB (X-Gen Pharmaceuticals Inc., Big Flats, NY) were evaluated using the well described neutropenic thigh infection model.[24] The study protocol was reviewed and approved by the Hartford Hospital Institutional Animal Care and Use Committee.

Briefly, female ICR mice weighing approximately 25 g were acquired from Harlan Sprague−Dawley, Inc. (Indianapolis, IN) and utilized throughout these experiments. Mice were rendered neutropenic with 100 and 150 mg/kg intraperitoneal injections of cyclophosphamide (Cytoxan; Bristol-Myers Squibb, Princeton, NJ) given 1 and 4 days prior to inoculation, respectively. Each thigh of the mice was inoculated with 10^7 colony forming units (CFU)/mL of the infecting organism. For these studies, *P. aeruginosa* 1401 (PA01) and 1402 (UC12120) were utilized. **5x** and PMB minimum inhibitory concentrations were 0.5 mg/L for both organisms as determined using the broth microdilution methodology described by the Clinical and Laboratory Standards Institute. Two hours after inoculation, groups of three mice were administered subcutaneous doses of **5x** and PMB as total daily doses of 5−400 mg/kg given 1, 2 (q12h) or 4 (q6h) times over a 24 h period. After 24 h, mice were euthanized by CO_2 asphyxiation followed by cervical dislocation; thigh tissue was harvested, homogenized in normal saline, and bacterial density quantified using serial dilution and plating techniques. Efficacy was evaluated as the change in bacterial density in treated mice as compared with 0 h (initiation of treatment) control animals.

Pharmacokinetic studies of **5x** and PMB were conducted in infected, neutropenic mice. For these analyses, mice were infected and inoculated as described above. Next animals were administered single subcutaneous doses of the test compounds ranging from 12.5 to 75 mg/kg. Groups of six mice were euthanized as described above, and blood was collected via cardiac puncture at eight time points over a 12 h interval. Plasma was collected via centrifugation, and samples were stored at −80 °C until concentration determination via a validated liquid chromatography−mass spectrometry assay.

Pharmacokinetic parameters for single doses of **5x** and PMB were calculated by nonlinear least-squares techniques (WinNonlin version 5.0.1, Pharsight, Mountain View, CA). The mean pharmacokinetic parameters derived from single dose studies were used to construct concentration−time profiles for all doses evaluated in the bacterial density studies. The area under the concentration−time profile (AUC) was calculated using the trapezoidal rule. For free drug assessments, protein binding values of 46% and 83% were utilized for **5x** and PMB, respectively.

For pharmacodynamic analyses, composite plots of the change in $\log_{10}$CFU for both *P. aeruginosa* isolates versus *f*AUC/MIC (ratio of the *f*AUC to MIC of the infecting organism) were constructed and fit to a sigmoidal E_{max} inhibitory model with baseline effects (WinNonlin version 5.0.1, Pharsight, Mountain View, CA). The exposure index required for stasis, 1 log reduction, 50% of maximal efficacy (EI_{50}), and 80% of maximal (EI_{80}) efficacy, was calculated from the respective E_{max} profile for **5x** and PMB.

AUTHOR INFORMATION

Corresponding Author

*Phone: 617-551-3513. E-mail: thomas.v.magee@pfizer.com.

Present Addresses

[#]Pfizer Cardiovascular, Metabolic, and Endocrine Diseases (CVMED) Chemistry, Cambridge, Massachusetts 02139, United States.

[▽]Astra-Zeneca Research Center, Waltham, Massachusetts 02451, United States.

[○]Cubist Pharmaceuticals, 65 Hayden Avenue, Lexington, Massachusetts 02421, United States.

Notes

The authors declare no competing financial interest.

■ ACKNOWLEDGMENTS

We thank Justin G. Stroh for performing high resolution mass spectrometry analyses and the staff of the Center for Anti-Infective Research and Development for their assistance with in vivo experimentation.

■ ABBREVIATIONS USED

PMB, polymyxin B; PMBN, polymyxin B nonapeptide; LPS, lipopolysaccharide; MIC, minimum inhibitory concentration; MBC, minimum bactericidal concentration; hRPTEC, human renal proximal tubule epithelial cell; TC_{50}, toxicity concentration 50%; Dab, L-2,4-diaminobutyric acid; Dap, L-2,3-diaminoproprionic acid; PA, *Pseudomonas aeruginosa*; AB, *Acinetobacter baumannii*; KP, *Klebsiella pneumoniae*; EC, *Escherichia coli*; hRPTEC, human renal proximal tubule epithelial cell; AA, amino acid; KDO, 3-deoxy-D-mannooctulosonic acid; DCM, dichloromethane; Fmoc, fluorenylmethyloxycarbonyl; Dde, 1-(4,4-dimethyl-2,6-dioxacyclohexylidene)-ethyl; ETS, exploratory toxicity study

■ REFERENCES

(1) (a) Maragakis, L. L. Recognition and prevention of multidrug-resistant Gram-negative bacteria in the intensive care unit. *Crit. Care Med.* **2010**, *38* (Suppl), S345−S351. (b) Munoz-Price, L. S.; Weinstein, R. A. Acinetobacter Infection. *N. Engl. J. Med.* **2008**, *358*, 1271−1281. (c) Falagas, M. E.; Bliziotis, I. A. Pandrug-resistant Gram-negative bacteria: the dawn of the post-antibiotic era? *Int. J. Antimicrob. Agents* **2007**, *29*, 630−636. (d) Gootz, T. D.; Marra, A. *Acinetobacter baumannii*: an emerging multidrug-resistant threat. *Expert Rev. Anti-Infect. Ther.* **2008**, *6*, 309−325. (e) Talbot, G. H. What is in the pipeline for Gram-negative pathogens? *Expert Rev. Anti-Infect. Ther.* **2008**, *6*, 39−49.

(2) (a) Nation, R. L.; Li, J. Colistin in the 21st century. *Curr. Opin. Infect. Dis.* **2009**, *22*, 535−543. (b) Landman, D.; Georgescu, C.; Martin, D. A.; Quale, J. Polymyxins Revisited. *Clin. Microbiol. Rev.* **2008**, 449−465. (c) Sarkar, S.; DeSantis, E. R. H.; Kuper, J. Resurgence of colistin use. *Am. J. Health-Syst. Pharm.* **2007**, *64*, 2462−2466. (d) Li, J.; Nation, R. L.; Turnidge, J. D.; Milne, R. W.; Coulthard, K.; Rayner, C. R.; Paterson, D. L. Colistin: the re-emerging antibiotic for multidrug-resistant Gram-negative bacterial infections. *Lancet Infect. Dis.* **2006**, *6*, 589−601. (e) Yuan, Z.; Tam, V. H. Polymyxin B: a new strategy for multidrug-resistant Gram-negative organisms. *Expert Opin. Invest. Drugs* **2008**, *17*, 661−668. (f) Zavascki, A. P.; Goldani, L. Z.; Li, J.; Nation, R. L. Polymyxin B for the treatment of multidrug-resistant pathogens: a critical review. *J. Antimicrob. Chemother.* **2007**, *60*, 1206−1215.

(3) (a) Benedict, R. G.; Langlykke, A. F. Antibiotic activity of *Bacillus polymyxa*. *J. Bacteriol.* **1947**, *54*, 24−25. (b) Ainsworth, G. C.; Brown, A. M.; Brownlee, G. 'Aerosporin', an antibiotic produced by *Bacillus aerosporus* Greer. *Nature* **1947**, *160*, 263.

(4) The (*S*)-6-methyl octanoyl side chain containing component is either polymyxin B1 or colistin A, which make up ∼65% of polymyxin B and colistin, respectively. Both mixtures contain a substantial percentage (∼15%) of 6-methyl heptanoyl side chain, known as polymyxin B2 or colistin B, respectively. There are several minor components as well. For analytical methods and more detailed component analysis, see (a) Kang, J. W.; Van Schepdael, A.; Orwa, J. A.; Roets, E.; Hoogmartens, J. Analysis of polymyxin B sulfate by capillary zone electrophoresis with cyclodextrin as additive. Method development and validation. *J. Chromatogr.* **2000**, *879*, 211−218. (b) Orwa, J. A.; Govaerts, C.; Busson, R.; Roets, E.; Van Schepdael, A.; Hoogmartens, J. Isolation and Structural Characterization of Colistin Components. *J. Antibiot.* **2001**, *54*, 595−599. (c) Orwa, J. A.; Van Gerven, A.; Roets, E.; Hoogmartens, J. Development and Validation of a Liquid Chromatography Method for Analysis of Colistin Sulphate. *Chromatographia* **2000**, *51*, 433−436.

(5) The prodrug is known as either colistimethate sodium, colistin methanesulfonate, or simply CMS. Each of the five γ amine nitrogens of the Dab residues at positions 1, 3, 5, 8, and 9 has a methanosulfonate moiety which decomposes in serum to the corresponding free base. See Gobin, P.; Lemaitre, F.; Marchand, S.; Couet, W.; Olivier, J.-C. Assay of colistin and colistin methanesulfonate in plasma and urine by liquid chromatography−tandem mass spectrometry. *Antimicrob. Agents Chemother.* **2010**, *54*, 1941−1948.

(6) Molina, J.; Cordero, E.; Pachon, J. New information about the polymyxin/colistin class of antibiotics. *Expert Opin. Pharmacother.* **2009**, *10*, 2811−2828.

(7) (a) HsuChen, C.-C.; Feingold, D. S. The mechanism of polymyxin B action and selectivity toward biological membranes. *Biochem.* **1973**, *12*, 2105−2111. (b) Mares, J.; Kumaran, S.; Gobbo, M.; Zerbe, O. Interactions of lipopolysaccharide and polymyxin studied by NMR spectroscopy. *J. Biol. Chem.* **2009**, *284*, 11498−11506. (c) Srimal, S.; Surolia, N.; Balasubramanian, S.; Surolia, A. Titration calorimetric studies to elucidate the specificity of the interactions of polymyxin B with lipopolysaccharides and lipid A. *Biochem. J.* **1996**, *315*, 679−686. (d) Bruch, M. D.; Cajal, Y.; Koh, J. T.; Jain, M. K. Higher-order structure of polymyxin B: the functional significance. *J. Am. Chem. Soc.* **1999**, *121*, 11993−12004. (e) Bhattacharjya, S.; David, S. A.; Mathan, V. I.; Balaram, P. Polymyxin B nonapeptide: conformations in water and in lipopolysaccharide-bound state determined by two-dimensional NMR and molecular dynamics. *Biopolymers* **1997**, *41*, 251−265. (f) Pristovsek, P.; Kidric, J. Solution structure of polymyxins B and E and effect of binding to lipopolysaccharide: an NMR and molecular modeling study. *J. Med. Chem.* **1999**, *42*, 4606−4613. (g) Garidel, P.; Howe, J.; Brandenburg, K. Thermodynamic analysis of the interaction of lipopolysaccharides with cationic compounds. *Eng. Life Sci.* **2008**, *8*, 523−529.

(8) (a) Clausell, A.; Garcia-Subirats, M.; Pujol, M.; Busquets, M. A.; Rabanal, F.; Cajal, Y. Gram-negative outer and inner membrane models: insertion of cyclic cationic lipopeptides. *J. Phys. Chem. B* **2007**, *111*, 551−563. (b) Clausell, A.; Rabanal, F.; Garcia-Subirats, M.; Alsina, M. A.; Cajal, Y. Membrane association and contact formation by a synthetic analogue of polymyxin B and its fluorescent derivatives. *J. Phys. Chem. B* **2006**, *110*, 4465−4471. (c) Clausell, A.; Rabanal, F.; Garcia-Subirats, M.; Alsina, M. A.; Cajal, Y. Synthesis and membrane action of polymyxin B analogues. *Luminescence* **2005**, *20*, 117−123. (d) Clausell, A.; Busquets, M. A.; Pujol, M.; Alsina, A.; Cajal, Y. Polymyxin B−lipid interactions in Langmuir−Blodgett monolayers of *Escherichia coli* lipids: a thermodynamic and atomic force microscopy study. *Biopolymers* **2004**, *75*, 480−490. (e) Oh, J.-T.; Van Dyk, T. K.; Cajal, Y.; Dhurjati, P. S.; Sasser, M.; Jain, M. K. Osmotic stress in viable *Escherichia coli* as the basis for the antibiotic response by polymyxin B. *Biochem. Biophys. Res. Commun.* **1998**, *246*, 619−623. (f) Cajal, Y.; Rogers, J.; Berg, O. G.; Jain, M. K. Intermembrane molecular contacts by polymyxin B mediate exchange of phospholipids. *Biochemistry* **1996**, *35*, 299−308. (g) Cajal, Y.; Ghanta, J.; Easwaran, K.; Surolia, A.; Jain, M. K. Specificity for the exchange of phospholipids through polymyxin B mediated intermembrane molecular contacts. *Biochemistry* **1996**, *35*, 5684−5695. (h) Clausell, A.; Pujol, M.; Alsina, M. A.; Cajal, Y. Influence of polymyxins on the structural dynamics of *Escherichia coli* lipid membranes. *Talanta* **2003**, *60*, 225−234.

(9) For an excellent review see: Velkov, T.; Thompson, P. E.; Nation, R. L.; Li, J. Structure−activity relationships of polymyxin antibiotics. *J. Med. Chem.* **2010**, *53*, 1898−1916.

(10) (a) Li, J.; Nation, R. L.; Turnidge, J. D.; Milne, R. W.; Coulthard, K.; Rayner, C. R.; Paterson, D. I. Colitsin: the re-emerging antibiotic for multi-drug resistant Gram-negative bacterial infections. *Lancet Infect. Dis.* **2006**, *6*, 589−601. (b) Falagas, M. E.; Rafailidis, P. I.; Matthaiou, D. K.; Virtzili, S.; Nikita, D.; Michalopoulos, A. *Int. J. Antimicrob. Agents* **2008**, *32*, 450−454. (c) Falagas, M. E.; Kasiakou, S. K. Toxicity of polymyxins: a systematic review of the evidence from old and recent studies. *Crit. Care* **2006**, *10*, R27. (d) Hartzell, J. D.; Neff, R.; Ake, J.; Howard, R.; Olson, S.; Paolino, K.; Vishnepolsky, M.; Weinrob, A.; Wortmann, G. Nephrotoxicity associated with intra-

venous colistin (colistimethate sodium) treatment at a tertiary care medical center. *Clin. Infect. Dis.* **2009**, *48*, 1724−1728. (e) Kim, J.; Lee, K.-H.; Yoo, S.; Pai, H. Clinical characteristics and risk factors of colistin-induced nephrotoxicity. *Int. J. Antimicrob. Agents* **2009**, *34*, 434−438. (f) Ramasubban, S.; Majumdar, A.; Das, P. S. Safety and efficacy of polymyxin B in multidrug resistant Gram-negative severe sepsis and septic shock. *Indian J. Crit. Care Med.* **2008**, *12*, 153−157. (g) Mendes, C. A. C.; Cordeiro, J. A.; Burdmann, E. A. Prevalence and risk factors for acute kidney injury associated with parenteral polymyxin B use. *Ann. Pharmacother.* **2009**, *43*, 1948−1955. (h) Santamaria, C.; Mykietiuk, A.; Temporiti, E.; Stryjewski, M. E.; Herrera, F.; Bonvehi, P. Nephrotoxicity associated with the use of intravenous colistin. *Scand. J. Infect. Dis.* **2009**, *41*, 767−769. (i) Ouderkirk, J. P.; Nord, J. A.; Turett, G. S.; Kislak, J. W. Polymyxin B nephrotoxicity and efficacy against nosocomial infections caused by multiresistant Gram-negative bacteria. *Antimicrob. Agents Chemother.* **2003**, *47*, 2659−2662. (j) Falagas, M. E.; Rizos, M.; Bliziotis, I. A.; Rellos, K.; Kasiakou, S. K.; Michalopoulos, A. Toxicity after prolonged (more than four weeks) administration of intravenous colistin. *BMC Infect. Dis.* **2005**, *5*, DOI: 10.1186/1471-2334-5-1. (k) Ma, Z.; Wang, J.; Nation, R. L.; Li, J.; Turnidge, J. D.; Coulthard, K.; Milne, R. W. Renal disposition of colistin in the isolated perfused rat kidney. *Antimicrob. Agents Chemother.* **2009**, *53*, 2857−2864.

(11) (a) Vaara, M.; Vaara, T. Structure−activity studies on novel polymyxin derivatives that carry only three positive charges. *Peptides* **2010**, *31*, 2318−2321. (b) Vaara, M.; Siikanen, O.; Apajalahti, J.; Fox, J.; Frimodt-Moller, N.; He, H.; Poudyal, A.; Li, J.; Nation, R. L.; Vaara, T. A novel polymyxin derivative that lacks the fatty acid tail and carries only three positive charges has strong synergism with agents excluded by the intact outer membrane. *Antimicrob. Agents Chemother.* **2010**, *54*, 3341−3346. (c) Lundberg, C. V.; Vaara, T.; Frimodt-Moller, N.; Vaara, M. Novel polymyxin derivatives are effective in treating experimental *Escherichia coli* peritoneal infection in mice. *J. Antimicrob. Chemother.* **2010**, *65*, 981−985. (d) Vaara, M.; Vaara, T. Polymyxin derivatives and uses thereof. World Patent Application WO 2008/017734, 2008. (e) Vaara, M.; Fox, J.; Loidl, G.; Siikanen, O.; Apajalahti, J.; Hansen, F.; Frimodt-Moller, N.; Nagai, J.; Takano, M.; Vaara, T. Novel polymyxin derivatives carrying only three positive charges are effective antibacterial agents. *Antimicrob. Agents Chemother.* **2008**, *52*, 3229−3236.

(12) O'Dowd, H.; Kim, B.; Margolis, P.; Wang, W.; Wu, C.; Lopez, S. L.; Blais, J. Preparation of tetra-Boc-protected polymyxin B nonapeptide. *Tetrahedron Lett.* **2007**, *48*, 2003−2005.

(13) Viljanen, P.; Vaara, M. Susceptibility of Gram-Negative Bacteria to Polymyxin B Nonapeptide. *Antimicrob. Agents Chemother.* **1984**, *25*, 701−705.

(14) Sato, Y.; Shindo, M.; Sakura, N.; Uchida, Y.; Kato, I. Novel *des*-fatty acyl-polymyxin B derivatives with *Pseudomonas aeruginosa*-specific antimicrobial activity. *Chem. Pharm. Bull.* **2011**, *59*, 597−602.

(15) Leese, R. A. Antibiotic compositions for the treatment of Gram negative infections. United States Patent Application US 2010/0160215, 2010.

(16) Li, J.; Velkov, T.; Nation, R. L.; Thompson, P. E. Antimicrobial compounds. World Patent Application WO 2010/130007, 2010.

(17) (a) Beceiro, A.; Llobet, E.; Aranda, J.; Bengoechea, J. A.; Doumith, M.; Hornsey, M.; Dhanji, H.; Chart, H.; Bou, G.; Livermore, D. M.; Woodford, N. Phosphoethanolamine Modification of Lipid A in Colistin-Resistant Variants of *Acinetobacter baumannii* Mediated by the *pmrAB* Two-Component Regulatory System. *Antimicrob. Agents Chemother.* **2011**, *55*, 3370−3379. (b) Moffatt, J. H.; Harper, M.; Adler, B.; Nation, R. L.; Li, J.; Boyce, J. D. Insertion Sequence IS*Aba11* Is Involved in Colistin Resistance and Loss of Lipopolysaccharide in *Acinetobacter baumannii*. *Antimicrob. Agents Chemother.* **2011**, *55*, 3022−3024. (c) Lee, J.-Y.; Song, J.-H.; Ko, K. S. Identification of Nonclonal *Pseudomonas aeruginosa* Isolates with Reduced Colistin Susceptibility in Korea. *Microb. Drug Resist.* **2011**, *17*, 299−304.

(18) In many pathogenic species, the major PMB resistance mechanism involves the alteration of lipid A such that the overall net negative charge of lipopolysaccharide is reduced, thereby decreasing the charge attraction from positively charged PMB. This modification, mediated by the products of the *arnBCADTEF* locus in *P. aeruginosa*, is controlled by the PmrAB two-component regulatory system.[1] To identify analogues that had activity despite this mechanism, we included the strain PA-1646, which shows a PMB-resistant phenotype as a result of a mutated PmrAB. This mutation renders this two-component regulatory system constitutively active, meaning that the modified lipid A moiety is constantly expressed on the cell surface. We confirmed this phenotype both by direct DNA sequencing of the *pmrAB* locus in PA-1646 and also by generating a site-specific *arnBCADTEF* deletion mutant within this clinical strain. This mutant, unlike the wild-type, displays a fully PMB susceptible phenotype (data not shown), indicating that the mechanism of resistance in this strain is mediated by this modification operon. As a result, any activity displayed by our analogs against this strain suggest that they maintain their effectiveness against a *P. aeruginosa* strain expressing the major first-step resistance mutation in this species.

(19) Developed in collaboration with CeeTox, Inc., Kalamazoo MI 49008.

(20) Meredith, J. J.; Dufour, A.; Bruch, M. D. Comparison of the Structure and Dynamics of the Antibiotic Peptide Polymyxin B and the Inactive Nonapeptide in Aqueous Trifluoroethanol by NMR Spectroscopy. *J. Phys. Chem. B* **2009**, *113*, 544−551.

(21) The data for this assay showed good reproducibility. For example: PMB (n = 29 tests) the hRPTEC TC_{50} = 22 ± 6 mM and, at the higher end, for **5p** (n = 30 tests) the hRPTEC TC_{50} = 82 ± 14 mM.

(22) We were unable to generate a TC_{50} with this analog even when tested at higher concentrations (only 10% inhibition seen at 300 mM).

(23) Lesions were graded from 1 to 4 for minimal, mild, moderate, and marked respectively and averaged over the dose group.

(24) Kim, A.; Banevicius, M. A.; Nicolau, D. P. In vivo pharmacodynamic profiling of doripenem against *Pseudomonas aeruginosa* by simulating human exposures. *Antimicrob. Agents Chemother.* **2008**, *52*, 2497−2502.

(25) Chen, J. M.; Li, Z. B.; Magee, T. V.; Martinez, C. A. Polymyxin derivatives useful as antibacterial agents. PCT Int. Appl. WO2012168820, 2012; *Chem. Abstr.* **2012**, 1819188.